

A new habitat map of the Lena Delta in Arctic Siberia based on field and remote sensing datasets

Simeon Lisovski^{1,*}, Alexandra Runge^{2,*}, Iuliia Shevtsova¹, Nele Landgraf³, Anne Morgenstern²,
Ronald Reagan Okoth^{1,4}, Matthias Fuchs², Nikolay Lashchinskiy^{5,6}, Carl Stadie^{2,7}, Alison
Beamish⁸, Ulrike Herzschuh^{1,9,10}, Guido Grosse^{1,11}, Birgit Heim¹

6

^{*} Both authors contributed equally

¹ Alfred Wegener Institute Helmholtz Centre for Polar and Marine Research, Polar Terrestrial
Environmental Systems, 14473 Potsdam, Germany

² Alfred Wegener Institute Helmholtz Centre for Polar and Marine Research, Permafrost Research, 14473
Potsdam, Germany

³ Humboldt University, Department of Geosciences, 12489 Berlin, Germany

⁴ Julius-Maximilians Universität Würzburg, Institute of Geography and Geology, Oswald-Külpe-Weg 86,
97074 Würzburg, Germany

⁵ Central Siberian Botanical Garden, Siberian Branch, Russian Academy of Sciences, Novosibirsk,
630090 Russia

⁶ Trofimuk Institute of Petroleum Geology and Geophysics, Siberian Branch, Russian Academy of
Sciences, Novosibirsk, 630090 Russia

⁷ University of Greifswald, Institute for Geography and Geology, Germany (current address: University of
Copenhagen, Department of Earth Science and Nature Management, Denmark)

⁸ GFZ German Research Centre for Geosciences, Helmholtz Centre Potsdam.

⁹ University of Potsdam, Institute of Environmental Sciences & Geography, Karl-Liebknecht-Str. 24-25,
14476 Potsdam, Germany

¹⁰ University of Potsdam, Institute of Biochemistry and Biology, Karl-Liebknecht-Str. 24-25, 14476
Potsdam, Germany

¹¹ University of Potsdam, Institute of Geosciences, Karl-Liebknecht-Str. 24-25, 14476 Potsdam, Germany

Correspondence to: Simeon Lisovski (Simeon.Lisovski@awi.de), Alexandra Runge
(alexandra.runge@gfz.de), Birgit Heim (birgit.heim@awi.de)

29

Abstract. The Lena Delta is the largest river delta in the Arctic (about 30 000 km²) and prone to rapid changes due to climate warming, associated cryosphere loss and ecological shifts. The delta is characterized by ice-rich permafrost landscapes and consists of geologically and geomorphologically diverse terraces covered with tundra vegetation and of active floodplains, featuring approximately 6 500 km of channels and over 30 000 lakes. Because of its broad landscape and habitat diversity the delta is a biodiversity hotspot with high numbers of nesting and breeding migratory birds, fish, caribou and other mammals and was designated a State Nature Reserve in 1995. Characterizing plant composition, above ground biomass and application of field spectroscopy was a major focus of a 2018 expedition to the delta. These field data collections were linked to Sentinel-2 satellite data to upscale local patterns in land cover and associated habitats to the entire delta. Here, we describe multiple field datasets collected in the Lena Delta during summer 2018 including foliage projective cover (Shevtsova et al., 2021a), above ground biomass (Shevtsova et al., 2021b), and hyperspectral field measurements (Runge et al., 2022). We further describe a detailed Sentinel-2 satellite image-based classification of habitats for the central Lena Delta (Landgraf et al., 2022), an upscaled classification for the entire Lena Delta (Lisovski et al., 2022), as well as a synthesis product for disturbance regimes (Heim and Lisovski, 2023) in the delta that is based on the classification, the described datasets, and field expertise. We present context and detailed methods of these openly available datasets and show how their combined use can improve our understanding of the rapidly changing Arctic tundra system. The new Lena Delta habitat classification represents a first baseline against which future observations can be compared. The link between such detailed habitat classifications and disturbance regime may provide a better understanding of how Arctic lowland landscapes will respond to climate change and how this will impact land surface processes.

1 Introduction

Global warming has profound impacts on the polar regions (Serreze and Barry, 2011; Overland et al., 2019). Rapidly increasing temperatures and changing precipitation regimes result in declining sea ice, warming and thawing of permafrost, more frequent tundra fires, and changes in vegetation (e.g., Biskaborn et al., 2019; Hu et al., 2015; Mauclet et al., 2022; Box et al., 2019; Amap, 2021). The Arctic tundra biome, which is normally characterized by harsh living conditions and nutrient-deficiency, has experienced rapid phenological shifts, such as earlier green-up in spring, which is also associated with increasing shrubification rates (Mekonnen et al., 2021). Shifts in plant communities are also driven by changing nutrient availability in permafrost soils (Mekonnen et al., 2021; Mauclet et al., 2022), affecting the net primary productivity of tundra ecosystems.

Deleted: , <https://doi.pangaea.de/10.1594/PANGAEA.945982>....

Deleted: , <https://doi.org/10.5281/zenodo.7575691>

65 Satellite-derived remote sensing can provide large-scale assessments of Arctic vegetation cover and
66 changes therein (Bartsch et al., 2016). For example, the Circumpolar Arctic Vegetation Map (CAVM)
67 project, from the Conservation of Arctic Flora and Fauna working group (CAFF), provided a first
68 panarctic vegetation composition map based on Advanced Very-High Resolution Radiometer
69 (AVHRR) false-color infrared (CIR) composites at a 1:4 million map scale (Walker, 1998; Raynolds
70 et al., 2019). Later, higher resolution land cover maps became available across all spatial scales
71 from national and international efforts such as the NASA Arctic-Boreal Vulnerability Experiment
72 (ABOVE) providing open-source data collections from boreal and arctic regions (ABOVE Science
73 Definition Team, 2014) specifically for Alaska, Canada, Northern Europe, and Western Siberia,
74 providing a better bridge to field measurements. Such products greatly assist in monitoring and
75 upscaling of patterns and dynamics of soil properties, land-atmosphere fluxes, ecosystem states,
76 and changes therein (e.g., Walker, 1998; Beamish et al., 2020; Berner et al., 2020; Sweeney et al.,
77 2022; Macander et al., 2022; Endsley et al., 2022). For selected Eastern Siberian tundra regions,
78 land cover maps have been produced (e.g., Veremeeva and Gubin, 2009; Bartsch et al., 2019;
79 Schneider et al., 2009), including the Lena Delta (Bartsch et al., 2019; Schneider et al., 2009).

80 Arctic river deltas represent distinct and vulnerable geomorphological and ecological regions at the
81 marine-terrestrial boundary. River deltas have been studied intensively to better understand land
82 cover and vegetation compositions (Jorgenson, 2000; Schneider et al., 2009; Frost et al., 2020;
83 Bartsch et al., 2020), carbon pools and fluxes (Bartlett et al., 1992; Schneider et al., 2009; Sachs et
84 al., 2008; Rossger et al., 2022), and land cover change caused by climate change impacts
85 (Jorgenson, 2000; Pisaric et al., 2011; Lantz et al., 2015; Nitze and Grosse, 2016; Vulis et al., 2021;
86 Juhls et al., 2021). With diverse habitats, Arctic river deltas are biodiversity hotspots (Gilg et al.,
87 2000), but at the same time are prone to rapid changes (Walker, 1998; Overeem et al., 2022). Arctic
88 deltas are affected by permafrost thaw (e.g., Pisaric et al., 2011; Nitze and Grosse, 2016; Vulis et
89 al., 2021), sea ice loss (Overeem et al., 2022), and increased sediment transport and organic load
90 during spring floods (Piliouras and Rowland, 2020; Juhls et al., 2021). Arctic river deltas are very
91 dynamic systems and high-resolution habitat information from these biodiversity hotspots is needed
92 to assess and predict changes and implications of Arctic warming.

93 The Lena Delta is the largest Arctic river delta representing a typical lake-rich lowland permafrost
94 landscape (Grigoriev, 1993). Over the past decades, the central Lena Delta became a place of
95 intensive international research. In addition to long-term permafrost monitoring at the Research
96 Station Samoylov Island (Hubberten et al., 2006; Boike et al., 2019), extensive records on
97 meteorology, soil and ecosystem characteristics (Zibulski et al., 2016; Boike et al., 2019; Boike et al.,
98 2008), hydrology (Fedorova et al., 2015), and greenhouse gas fluxes (Rossger et al., 2022; Holl et

99 al., 2019) are available, setting an important benchmark for further assessments of changes in an
100 Arctic river delta. During the summer season of 2018, an extensive field campaign to the Lena Delta
101 led to an unprecedented amount of field datasets including vegetation cover recordings, above
102 ground biomass estimates, and spectral characterisation of the different vegetation/land cover units.
103 These in situ datasets provide improved thematic detail allowing the development of habitat
104 classifications. In 2009, Schneider et al. (2009) developed the first land cover classification map for
105 the entire delta at 30 m spatial resolution based on Landsat-7 ETM+ satellite summer images from
106 2000 and 2001 to quantify delta-wide methane emissions. The availability of Sentinel-2 (Sentinel-2)
107 Multispectral Instrument (MSI) data from two orbiting satellite missions since 2016 and 2017 provide
108 high quality multispectral satellite data with a higher spatial resolution in the Visible and Near
109 Infrared wavelength of up to 10 m, and of 20 m in the Red Edge and the Short- Wave Infrared
110 wavelength regions (Drusch et al., 2012, ESA 2015). Together with the extensive ground
111 observations from the Lena Delta in 2018 this enables an updated classification, using the higher
112 resolution Sentinel-2 images and improved thematic detail.

113 In the following study, field datasets as well as derived multispectral satellite images from the
114 summer season 2018 for the Lena Delta were used to provide 1) an updated data-driven framework
115 for plant communities and associated habitat classes in the Lena Delta, 2) a high-resolution habitat
116 mapping product for the entire delta, and 3) a disturbance regime map linked to habitat classes.
117 These datasets enhance our understanding of the Lena Delta system and will build a baseline and
118 framework for future spatio-temporal analysis of more detailed processes and changes within this
119 highly sensitive ecosystem.

120 2 Study Area

121 The Lena Delta is located in northeastern Siberia's continuous permafrost zone between 72° and
122 74°N and 123° to 130°E (Figure 1). With an area of about 30 000 km², it is the largest delta in the
123 Arctic and one of the largest in the world (Walker, 1998; Schneider et al., 2009). It is surrounded by
124 the Laptev Sea to the west, north, and east, and the Chekanovsky and Kharaulakh mountain ranges
125 border it to the south. The delta is characterized by numerous river channels and more than 1500
126 islands with a diverse geologic history (Grigoriev, 1993). Morphologically, the delta can be divided
127 into three distinct geomorphological main terraces (Grigoriev, 1993; Schwamborn et al., 2002). The
128 first main terrace, which comprises the Holocene fluvial terraces and the active floodplains, is the
129 youngest and most active part of the delta (Schwamborn et al., 2023), and covers most of the east-
130 northeastern areas as well as the southern and southwestern-most parts This main terrace
131 predominantly consists of ice wedge-polygonal tundra (Nitzbon et al., 2020) as well as of barren and

132 vegetated floodplain areas (e.g., Rossger et al., 2022). The second main terrace, located in the
133 northwestern part, contains mostly sandy, comparably well-drained soils with low ground-ice content
134 (Schwamborn et al., 2002; Ulrich et al., 2009). Large, mostly north-to-south oriented lakes and
135 depressions are abundant in this area (Morgenstern et al., 2008). The third and oldest main terrace
136 consists mainly of remnants of a Late Pleistocene accumulation plain with ice- and organic-rich
137 sediments (so-called Yedoma deposits) and is characterized by polygonal tundra with large ice
138 wedges, deep thermokarst lake basins, and thermo-erosional valleys (Morgenstern et al., 2011;
139 Morgenstern et al., 2021). The third terrace is found on islands in the southern delta region
140 (Schirrmeister et al., 2003; Schirrmeister et al., 2011). Permafrost in the area has a thickness of
141 about 500–600 m (Romanovskii and Hubberten, 2001). The active layer depth, i.e., the seasonally
142 thawing upper soil layer, on the first terrace is usually in the range of 30 to 50 cm and 80 to 120 cm
143 on the floodplains (Boike et al., 2019). The larger region is characterized by an Arctic continental
144 climate with low mean annual air temperatures of -13°C , a mean temperature in January of -32°C ,
145 and a mean temperature in July of 6.5°C . The mean annual precipitation is low and amounts to
146 about 190 mm (World Weather Information Service).

147 As part of past Russian-German expeditions to the Lena Delta, most research during the last two
148 decades has been carried out on the islands of Samoylov and Kurungnakh in the central delta
149 (Figure 1). Samoylov Island ($72^{\circ}22' \text{N}$, $126^{\circ}29' \text{E}$) covers an area of about 5 km^2 and is
150 representative of the first terrace together with an active floodplain (Boike et al., 2019; Boike et al.,
151 2008). The vegetation and soil types are diverse at local scales due to high lateral variability of the
152 polygonal microrelief consisting of drier polygon rims, and moist to wet polygonal depressions and
153 troughs (Nitzbon et al., 2020; Kienast and Tsherkasova, 2001). In contrast, Kurungnakh Island is
154 mainly composed of late Pleistocene Yedoma deposits that belong to the third delta terrace
155 (Grigoriev, 1993) with elevation up to 55 m above sea level (m a.s.l.) (Morgenstern et al., 2013).
156 Holocene cover deposits and peat-rich permafrost soils are distributed across the surface of the third
157 Lena River terrace and especially concentrated in the deep thermokarst basins called “alases”.
158 Alases are important landscape-forming features of the ice-rich Yedoma permafrost zone, which are
159 mainly caused by extensive melting of excess ground ice in the underlying permafrost (Van
160 Everdingen, 1998).

161

3 Datasets and methods

Several new datasets are presented for the Lena Delta that are spatially and thematically connected and support vegetation, habitat, and land cover applications for this region (Figure 1).

Two datasets feature field-measured vegetation data, providing information on foliage projective cover (Dataset 1) and above ground biomass (Dataset 2) recorded in the central Lena Delta in summer 2018 across 26 selected vegetation plot sites (supplementary Table S1, S2). The field plots of 30 x 30 m (900 m²) were chosen to be representative for typical vegetation communities (vascular plants, moss and lichen cover) as largely homogenous sites representative for the surrounding area. In addition, a total of 28 in-situ, canopy-level hyperspectral field measurements were acquired in 30 x 30 m plots with homogeneous vegetation or barren to partially vegetated areas (spectral reflectance field measurements; Dataset 3). Of the 28 hyperspectral measurements, 15 were conducted at the vegetation plot sites of Datasets 1,2 three measurements were repeated measurements to capture vegetation senescence, and at 10 spectrometry plots we conducted hyperspectral field measurements without floristic inventories but with detailed plot documentation. Based on expert knowledge, we defined representative habitat classes and identified homogeneous regions within the central Lena Delta to train and apply a classifier using a Sentinel-2 satellite image from summer 2018 (Dataset 4). Due to the high reliability of the central Lena Delta vegetation classification and positive evaluation by field experts, we used this vegetation classification as a training dataset for a robust classifier that was subsequently applied to a Sentinel-2 image mosaic for the entire Lena Delta for 2018 to develop a new Lena Delta habitat map (Dataset 5).

Finally, using the habitat classes, probability maps for exposed sandbars and water distribution, and information from the in-situ dataset (Datasets 1 & 2), we extrapolated a classification of disturbance regimes across the delta (Dataset 6) as an application example for the habitat classes.

3.1 Foliage projective cover (Dataset 1)

A detailed description of plant composition for the 26 vegetation plots of the 2018 expedition to the Lena Delta was compiled (see supplementary [Tables S1-3](#)). Prior to the field work, the approximate site locations were defined for establishing representative vegetation plots based on field knowledge and evaluation of Landsat and Sentinel-2 satellite imagery. The aim was to cover representative vegetation communities of the central delta. There are vegetation communities with large area coverage that show high homogeneity within larger areas (10s of meters). Therefore, at each site location, we defined a 30 x 30 m square plot with a homogeneous or repetitive vegetation composition that was also representative of the wider land surface serving as an Elementary

Deleted: table

Deleted: , S2, S3

196 Sampling Unit (ESU). ESUs according to the Committee on Earth Observing Satellites Working
197 Group on Calibration and Validation (Duncanson et al., 2021) serve as spatial training and
198 validation units representative for the land surface for quantitative and qualitative remote
199 sensing operations. In case of more patchy and heterogeneous vegetation structure we selected 30
200 x 30 m squares embedded in a minimum of 50 x 50 m square of the same vegetation composition.

201 The detailed floristic composition was recorded around the plot center in four successive rings of 50
202 cm diameter. In addition, the vegetation plot was mapped in detail from above with one Red-Green-
203 Blue (RGB) and one Red-Green-Near Infrared (RGNIR) MAPIR camera using telescope stick-based
204 field photography. The projective vegetation cover was recorded in at least three subplots (2 m x 2
205 m) within the plot. If the vegetation cover was highly homogenous three subplots were established.
206 In the case of moisture differences, e.g. in polygonal tundra with dry rims and moist to wet
207 depressions, we established higher numbers of subplots capturing moist as well as dry patches
208 (see, Figure 2 & 3 describing the concept). We compiled the floristic composition to foliage projective
209 cover by plant taxa on each 2 x 2 m subplot for the different canopy levels and extrapolated for the
210 30 m x 30 m plot. We used the RGB and NIR field photos to make an estimate on the share of moist
211 and dry surface area to calculate an averaged projective vegetation cover. The ring survey data was
212 not included in the plot average. The dataset of percentage foliage projective cover per vegetation
213 plot is published in PANGAEA (Shevtsova et al., 2021a,
214 <https://doi.pangaea.de/10.1594/PANGAEA.935875>).

215 3.2 Above ground plant biomass (Dataset 2)

216 Above-ground biomass (ABG) was sampled in the field in 25 of the 26 vegetation plots in 2018 (see
217 supplementary [Tables S1-3](#)). Within each 2 x 2 m subplot a 0.5 m x 0.5 m representative plot was
218 selected for ABG sampling. AGB sampling for moss and lichens was conducted within 0.1 m x 0.1 m
219 subplots inside the 0.5 m x 0.5 m subplots.

220 In total, 174 fresh AGB samples were collected and weighed in the field or subsequently at the
221 Samoylov research station. AGB samples with a weight exceeding 15 g were subsampled. The plant
222 samples were then dried for two to four days in a warm dry place and finally oven-dried for ca. 24
223 hours at a temperature of 60 °C before re-weighing. All AGB assessments per plant community type
224 were upscaled to the 30 m x 30 m plot in g/m² using the foliage projective cover data. The dataset of
225 AGB per vegetation plot has been published in PANGAEA (Shevtsova et al., 2021b,
226 <https://doi.pangaea.de/10.1594/PANGAEA.935923>).

227 3.3 Hyperspectral field measurements (Dataset 3)

Deleted: table

Deleted: , S2, S3

Deleted: <https://doi.pangaea.de/10.1594/PANGAEA.935923>)....

232 Hyperspectral field measurements were conducted in the central Lena Delta in August 2018 with the
 233 aim to collect surface reflectance spectra of different homogeneous land cover units across a variety
 234 of delta land surfaces and vegetation composition. In total, we collected 28 hyperspectral field
 235 measurements in homogeneous 30 x 30 m spectrometry plots (Table S5), with 15 of them equalling
 236 the vegetation plots across Samoylov and Kurungnakh islands (see Dataset 1 & 2 and
 237 supplementary Table S4), three as repeat measurements at the end of August to capture the change
 238 in spectral signature during senescence since the beginning of August and the remaining 10 field-
 239 spectroscopy plots focusing on non-vegetated areas such as sandy parts of the floodplain. We
 240 conducted the field-spectroscopy measurements with a Spectral Evolution SR-2500 field
 241 spectrometer with a 1.5 m Fiber Optic Cable. The instrument was calibrated to spectral radiance
 242 within a wavelength range of 350 to 2500 nm. Within the 30 x 30 m homogeneous spectrometry
 243 plots we acquired about 100 individual measurements, randomly scattered across the plot. Before
 244 and after each survey we conducted reference measurements by measuring the back reflected
 245 downwelling radiance from a Zenith Lite™ Diffuse Reflectance Target of 50% reflectivity to normalize
 246 to surface reflectance percentages per wavelength. The averaged individual measurements of the
 247 reflectance of each spectrometry plot was published in the PANGAEA data repository (Runge et al.,
 248 2022, <https://doi.pangaea.de/10.1594/PANGAEA.945982>).

Deleted: <https://doi.pangaea.de/10.1594/PANGAEA.945982>)....

249 3.4 Central Lena Delta habitat classification (Dataset 4)

250 3.4.1 Habitat classes

251 Based on the vegetation plots (Dataset 1 & 2) and from field knowledge, different habitat classes
 252 characterized by distinct plant communities, moisture regimes and soil properties were defined. Non-
 253 vegetated areas (e.g., sand) and water were added as additional classes using band thresholds
 254 (Table 1). During an iterative process within a Sentinel-2 based supervised classification, additional
 255 habitat classes that were not covered by the vegetation plots (Dataset 1 & 2) were added: i) The
 256 polygonal tundra complex could spectrally be separated into distinct classes related to different
 257 surface water abundance in the form of intra- and interpolygonal ponds, therefore, we implemented
 258 three different polygonal tundra complex classes, with up to 10%, 20%, 50% surface water cover
 259 respectively, and ii) one class of 'sparsely vegetated' representing the areas of transition zones
 260 between vegetated and barren. Table 1 provides details on habitat class descriptions and
 261 established methods to distinguish habitats.

262 3.4.2 Satellite data processing

265 The central Lena Delta habitat classification is based on one high quality cloudless Sentinel-2)
 266 image from August 6 in 2018, representing the late summer. The Sentinel-2 top of atmosphere
 267 reflectance (TOA) image data was processed by the German Space Agency DLR (B. Pflug, oral
 268 communication, 2019) to bottom of atmosphere (BOA) surface reflectance using the newest version
 269 of the atmospheric correction processor Sen2Cor later released as ESA Sen2Cor in 2020.
 270 Atmospheric correction processing was performed with the default rural aerosol model. All spectral
 271 bands were resampled to the 10 m pixel resolution bands. The 60 m pixel resolution bands (B1, B9,
 272 B10) that support atmospheric correction, but are not optimal for land surface classification, were
 273 removed. We added the normalized difference vegetation index (NDVI; $\text{NIR-RED} / \text{NIR} + \text{RED}$) to
 274 the band collection.

275 3.4.3 Central delta habitat classification

276 Sentinel-2 pixels from the 30 x 30 m ESUs (dataset 1, Shevtsova et al. 2021a), and additional
 277 polygonal shapefiles (Figure A3) defined by expert knowledge, led to a training dataset of 8 626
 278 labelled pixels for the habitat classification (labelled pixels are published in the Landgraf et al 2022a
 279 data collection). An independent test dataset of polygonal shapefiles with habitat annotation was
 280 delineated based on high resolution satellite and drone images, S-2 NDVI and SWIR bands and in
 281 areas that have been visited regularly during field expeditions (Figure A4).
 282 From the training dataset we randomly selected 4 313 pixels to train the classifier. We tested
 283 several classifiers and different selected band combinations (spectral bands and NDVI). Water
 284 (transparent to turbid) and sandbanks were omitted in the classification processing by masking them
 285 as inactive using a band threshold; the water mask was based on the NIR 10 m band 8 ($\text{NIR} < 0.02$)
 286 and the sand mask was based on the blue 10 m band 2 ($\text{Blue} > 0.07$, Table 1). The classification
 287 was tuned to depict vegetation composition and was qualitatively assessed well known to the
 288 classification developers. Best results for the habitat classification were obtained using a random
 289 forest classification with a band combination of all Sentinel-2 VIS, Red-Edge, NIR and SWIR bands,
 290 and the NDVI. The chosen classifier was able to distinguish between relevant classes (Table 1) and
 291 could even identify patchy spots of specific habitat classes. In addition to the defined water and sand
 292 classes, the final central Lena Delta classification contains 10 habitat classes (Table 1). The here
 293 defined central Lena Delta covers an area of 644.9 km² with a 55.2 % vegetation cover.

294 To assess the classification performance, we applied a cross-validation on a random selection of
 295 locations within the independent test dataset and used landscape descriptions at permafrost coring
 296 sites (Siewert et al. 2016 a,b,c) (Figure S 6). We used 34 locations that we could relate to categories
 297 such as polygonal tundra, wetlands, and sandy areas. These broad land cover categories matched
 298 well (Table S8). For the evaluation, 100 random points per pre-defined habitat class were selected
 299 from the test dataset. Based on a confusion matrix, the overall classification accuracy was 94.00 %

Deleted: polygons

Deleted: From those 8 626 pixels we randomly selected 50 % for the training and 50 % for validation. Polygons were defined by BH,

Deleted: RGB

Deleted: an independent

Deleted: the training pixels (50 %).

Deleted: (supplementary table S5),

Deleted: 96.78

(class-based accuracy and statistics shown in Table A1). More importantly, the accuracy was qualitatively tuned and evaluated based on ground-truthed knowledge of the development team. The published dataset of Landgraf et al. (2022, <https://doi.pangaea.de/10.1594/PANGAEA.945057>) provides the central Lena Delta habitat classification map, the ESUs and the polygons used to train the classifier. The training dataset includes data from 23 of the 26 vegetation plots (dataset 1). The dataset provides additional 69 ESUs defined with expert knowledge gathered during several field expeditions to the Lena Delta, labeled as pseudo ESUs for potential future investigations.

Deleted: However, this is partly due to autocorrelation resulting from pixel selection within polygons.

3.5 Lena Delta habitat classification (Dataset 5)

3.5.1 Lena Delta habitat classes

In order to extend the habitat classification map to the entire Lena Delta (29873.7 km²), we included all the habitat classes covering the central Lena Delta (dataset 4, Table 1). In addition, and based on expert knowledge as well as extensive visual satellite image investigations, we added one habitat class that is not present in the central Lena Delta: the second terrace in the northwest of the Lena Delta is lithologically and geomorphologically different from the other two terraces present in the central delta, and characterized by sandy substrates. In a hyperspectral CHRIS PROBA satellite-based geomorphological classification, Ulrich et al. (2009) described the second terrace featuring very dry elevated sandbanks, barren or poorly vegetated areas with isolated lichens, moss, herbs, dwarf shrubs or grasses (vegetation cover 0–60%, growth height: max. 20 cm, average active layer depth of 1 m on the upland plain with old, vegetation-arrested sand dunes). Based on photos taken at few locations in the field during past expeditions (see supplementary table S3) the habitat class shows well-drained areas dominated by sandy substrate and diverse, sparse vegetation cover; some areas are dominated by sedges, cotton grass and mosses with rare occurrences of lichens and dwarf shrubs, while some areas are dominated by the latter. Schneider et al. (2009) defined the same class as 'dry moss-, sedge- and dwarf shrub-dominated tundra (DMSD)'. We selected 35 ESUs for this habitat class characterized by high SWIR reflectance (Sentinel-2 band 11) due to dry land surface conditions. The habitat class was named 'dwarf shrub - herb communities' and was added as an additional habitat class to the training data set.

3.5.2 Satellite data processing

The Lena Delta habitat classification was based on a Sentinel-2 mosaic (top of atmosphere (TOA) reflectance, Google Earth Engine Dataset) with images taken of the area between June 1 and September 15, 2018. The images (N = 1685, distributed across 15 Sentinel-2 tiles) were filtered to discard images with cloud cover above 20%. A cloud mask was applied to the remaining 262

343 images, masking pixels where the quality band 'QA60' indicates clouds (band 10) or cirrus (band
344 11). All spectral bands with 20 m resolution were resampled to match the 10 m resolution bands.
345 Next, NDVI was computed (see 3.4) for each image and one high-quality mosaic of all images based
346 on the maximum NDVI value per pixel was produced representing a snapshot of the peak summer
347 vegetation period. Using the median NIR band values across the 262 cloud-masked images, we
348 classified water with a threshold of < 0.07 reflectance. The remaining non-vegetated areas defined
349 by a threshold of $NDVI < 0.4$ were classified as barren/sand. The water- and sand-masked image
350 mosaics were then used in the classification pipeline with the following bands: B2 (blue), B3 (green),
351 B4 (red), B5 (red edge 1), B6 (red edge 2), B7 (red edge 3), B8 (NIR), B11 (SWIR 1), B12 (SWIR 2),
352 and NDVI.

353 3.5.3 Lena Delta Habitat classification

354 From the central Lena Delta habitat classification (dataset 4) we sampled 7 500 random pixels to
355 train a random forest classifier (smileRandomForest in Google Earth Engine). In addition, we added
356 35 pixels from the ESUs selected within the 'dwarf shrub - herb communities' of the north-western
357 Lena Delta. Given the dominance of the 'dwarf shrub - herb communities' on the second terrace
358 (north-eastern part of the Lena Delta), the confidence of selecting correct training pixels for this
359 habitat was relatively high (see also Figure S7). Unfortunately, no vegetation recording or monitoring
360 schemes exist outside the central Lena Delta. The accuracy of the classification was quantified using
361 the independently defined shapefiles within the central Lena Delta (same dataset used to quantify
362 the accuracy of the central Lena Delta habitat classification, Figure A4 and Table S1). Based on a
363 confusion matrix, the overall classification accuracy was 85.06 % (class-based accuracy and
364 statistics shown in Table A2). Similar to the validation of the central Lena Delta habitat classification,
365 the results were carefully checked to make sure that large-scale pattern, e.g., differences between
366 the three terraces, are accurately separated, and that the highly repetitive structures within terraces
367 are also recognized by the classification (see Figures S6-S8).

368 Since the barren/sandy areas are highly dynamic with variable water levels mainly within (due to
369 flooding in spring and decreasing river flow during the summer season) but also across years
370 (discharge dynamics), we computed a sandbar probability map for the Lena Delta using cloud
371 masked Sentinel-2 (TOA reflectance) images between April 1 and October 15 from 2015 to 2021 (6
372 026 images). In each image, we labeled sandy pixels by $NDVI < 0.4$ AND $NDWI > 0.095$ AND $NIR <$
373 0.09 reflectance. Next, for each pixel in the Lena Delta, we computed the percentage of sandy pixels
374 across all images resulting in a sand probability map. The training dataset (random 7500 points, plus
375 35 points with label 'dwarf shrubs - herb communities'), the habitat classification, and the sand

Deleted: relative

Deleted: We thus lack format independent validation

Deleted: across

Deleted: .

Deleted: of the classifier

Deleted: on its training data (i.e., resubstitution error) was 96.47 %. Habitat class accuracy varied between 91.89 % and 100 % (see complete confusion matrix)

Deleted: sandbar

385 probability map was published in the PANGAEA repository (Figure 5, Lisovski et al., 2022,
386 <https://doi.pangaea.de/10.1594/PANGAEA.946407>).

Deleted: <https://doi.pangaea.de/10.1594/PANGAEA.946407>)....

387 3.6 Lena Delta disturbance regimes (Dataset 6)

388 The Lena Delta experiences different disturbance regimes, mapped and described in dataset 6.
389 Mainly annual flooding, but also local rapid thaw processes on the land surface of the terraces with
390 ice-rich permafrost, result in disturbance regimes forming distinct habitat classes (Table 2). The
391 floodplains experience seasonal flooding as a regularly occurring disturbance in spring after ice-
392 break up (the spring flood). Very high disturbance regimes due to the most intense scour, erosion
393 and sedimentation result in barren sandbanks or in early-stage plant communities equalling the
394 'sparsely vegetated' habitat class. The classes 'moist to wet sedge communities', 'wet sedge
395 communities', 'moist equisetum and shrubs', 'dry shrub communities', 'dry grass to wet sedge
396 communities' represent the mid to advanced successional stages on the floodplain within areas of
397 high disturbance that are also described as shifting habitat class (Stanford et al., 2005; Driscoll and
398 Hauer, 2019).

399 In contrast to the high disturbance regimes on the floodplain, habitats on the first, second and third
400 delta terraces are less extensively disturbed (low disturbance). In these areas typical mature-state
401 tundra plant communities are able to develop; 'polygonal tundra complex', 'tussock tundra', and
402 'dwarf shrub herb communities'. However, locally, high disturbance occurs by rapid thaw processes
403 of ice-rich permafrost on the first and third delta terraces with habitats characterized by mid to
404 advanced-stage plant succession; 'moist to wet sedge communities', 'wet sedge communities', 'dry
405 shrub communities', and 'dry grass to wet sedge' communities. Very high disturbance due to intense
406 rapid thaw processes occurs at eroding cliffs and lake margins, in steep valleys and actively
407 developing gullies resulting in barren surfaces with rims of sparsely vegetated transition zones.
408 Given the link between plant communities and flooding as well as rapid thaw processes, we
409 characterized the disturbance regimes for each habitat class (Table 2) and provide mapped
410 disturbance based on the habitat class of dataset 5 and the corresponding disturbance regime for
411 the entire Lena Delta (Figure 6, Heim and Lisovski, 2023, <https://doi.org/10.5281/zenodo.7575691>).

Deleted: dwarsh

412

4 Results and Discussion

We deliver a detailed description and associated data products of the most prominent habitat classes in the largest Arctic river delta, the Lena Delta. Supported by ecological field data of plant composition, hyperspectral field measurements from the same sites, and regional expert knowledge collected over decades, we develop a high-resolution Sentinel-2 based habitat map for the entire delta. The compiled datasets provide the necessary baseline for future investigations of the biochemical processes, ecological dynamics, and responses to global warming within the Arctic tundra system of the delta.

4.1 Habitat classes of the Lena Delta

Based on the floristic composition and biomass of the vegetation plots (Dataset 1, 2), the spectral properties from hyperspectral field measurements (Dataset 3) as well as expert knowledge, we defined 11 distinct habitat classes linked to different vegetation composition for the Lena Delta (Figure 4). The selected Sentinel-2 spectral bands and the derived NDVI values allow a separation of the habitat classes into two distinct groups (the first separation level between habitat classes in Figure 4a, 1st hierarchical level). Three habitat classes ('wet sedge communities', 'moist Equisetum and shrub communities', 'dry grass to wet sedge communities') formed in areas of high disturbance by rapid thaw processes and regular flooding represent a distinct cluster with highest vegetation vitality (high NDVI), and separated from the more stable and mature tundra communities ('polygonal tundra complex', 'dry (tussock) tundra', and 'dry dwarf-shrub and herb communities'), and the other successional plant communities ('moist to wet sedge complex', 'dry low shrub communities' and 'sparsely vegetated') all characterised by a lower NDVI range. The 'dry dwarf-shrub and herb communities' form a separate cluster with the least overlap with other habitat classes within the two-dimensional non-metric multidimensional scaling (NMDS) space (2nd hierarchical level, Figure 3a; Figure 4c) due to very low vegetation vitality and surface moisture (lowest NDVI, high red and SWIR reflectance). There are two remaining habitat classes on the 3rd and 4th hierarchical level, which are successional plant communities, the 'moist to wet sedge complex' and 'dry low shrub communities'. The separation on the 3rd and 4th hierarchical level is mainly driven by higher NDVI of these successional plant community classes in comparison with the mature state tundra plant communities with lower NDVI (Figure 4a-b). The 'dry grass to wet sedge communities' and the 'sparsely vegetated area' habitat class (not covered by vegetation plots but added during the classification process), show the largest overlap with the other habitat classes due to a high variability in vegetation cover, biomass and moisture. In general, the ordination method (Figure 4b) shows that distinct plant communities and the associated habitat classes are mostly separated by a biomass

449 gradient for which the NDVI is a good approximator. A further separation linked to potential spectral
450 proxies for biomass exists with the far red-edge and NIR bands (B6,7,8) but is less distinct than the
451 NDVI axis. Together with the SWIR (B11,12) the red (B4) and near red-edge (B5) bands, and less
452 strongly the blue and green bands (B2,3), the results indicate a habitat class separation based on
453 moisture, biomass and vegetation colour characteristics.

454 The vegetation plot selection was made in relation to the most typical habitats (e.g., Mueller-
455 Bombois and Ellenberg, 1974). For 15 of the 26 vegetation plots, we collected and provided
456 hyperspectral surface reflectance data (Runge et al., 2021). These measurements cover a variety of
457 landscape units including Yedoma uplands, floodplains (vegetated and non-vegetated), drained
458 thermokarst lake basins (old and recently drained), and areas covered by low shrub layers.
459 Comparing the hyperspectral surface reflectance with multispectral Sentinel-2 data, we found
460 commonalities in the discrimination of habitat classes along moisture gradients. Unfortunately, the
461 hyperspectral field measurements do not cover the biomass gradient. Plot measurements with the
462 field spectrometer are conducted with the hand-held instrument held at shoulder height, hence it was
463 not possible to acquire field spectroscopy measurements in disturbed patches with tall shrubs or
464 very sloped terrain. This highlights the difficulty in deriving high spectral resolution surface
465 reflectance measurements representative of fine scale differences between Arctic tundra habitat
466 classes if the plot properties become too challenging to measure.

467 In general, mature-state tundra plant communities have relatively similar spectral properties due to
468 low vascular plant cover (e.g., Beamish et al., 2017). In addition, the tundra vegetation communities
469 contain a wide range of accessory pigment composition (carotenoids and anthocyanins) that result in
470 a very similar spectral response (Beamish et al., 2018). Only the highly disturbed communities such
471 as wetlands or areas with tall shrubs are more spectrally distinct due to a high NIR reflectance
472 plateau (Buchhorn et al., 2013). Since the hyperspectral field measurements provide a higher spatial
473 resolution and thus also a measure of variability within areas of the same general habitat type, we
474 consider the measurements valuable for applications that aim at analysing ecological and
475 biochemical processes within distinct habitats in more detail.

476 **4.2 Sentinel-2 based habitat classification**

477 Based on the identified habitat classes (Table 1) we applied a random forest classifier to map habitat
478 classes in the central Lena Delta and subsequently in the entire Lena Delta. Both maps represent
479 the summer season of 2018 for which we could use a sufficient number of satellite images with low
480 cloud cover.

481 The Lena Delta habitat map shows the ice-rich first and third terraces mainly covered by i) the
482 'polygonal tundra complex' due to impeded drainage on the terrace plateaus and by ii) drier tundra
483 communities on well drained areas due to older degraded permafrost forms (detailed description in
484 Morgenstern et al., 2008, 2011). On the second terrace, the classified 'dry dwarf shrub and herb
485 communities' occur well separated from the moist habitat classes covering the floor of the alases.
486 On the floodplains, the rich mosaic outlines a wide spectrum of very diverse classes, the dry versus
487 moist and wet substrate habitats, in the active delta area.

488 Polygonal tundra is characterized by high spatial heterogeneity; at the decimeter to meter-scale
489 plant composition and diversity is defined by the polygonal microrelief and water level (Whitaker and
490 Woodwell, 1968; Forman and Godron, 1981; Zibulski et al., 2016; Nitzbon et al., 2020, Siewert et al.,
491 2021). Therefore, within a single Sentinel-2 pixel, dry polygonal rims, moist slopes, wet patches and
492 surface water can all be present. The spatial resolution of Sentinel-2 cannot capture the meter-scale,
493 but captures the heterogeneity between the different surface water contributions of the 'polygonal
494 tundra complex' on the first and third terrace. In the Lena Delta, the 'polygonal tundra complex with
495 up to 50% surface water' represents the dominant habitat class with 25% of the delta area (about 7
496 434 km²). All other habitat classes represent 1-6% of the delta area with 'dwarf shrub-herb
497 communities' and 'moist to wet sedge complex' reaching 5.4% and 5.9%, respectively (Figure 6).
498 Based on the summer Sentinel-2 mosaic, the classes 'Water' and 'Sand' cover more than 40% of the
499 delta. However, those two classes are extremely variable within and across years, depending on the
500 river water level during image acquisition time. To provide information on this variability, we
501 calculated how often each pixel in the delta (cloud free Sentinel-2 pixels from 2015 to 2022) was
502 classified as sand (threshold approach). This led to an additional sand probability layer with values
503 between 0-100%.

504 Despite extensive research within the area, only a few classification products are available for the
505 Lena Delta. The new Lena Delta classification is a high-resolution (Sentinel-2, 10 m) map that
506 focuses on the delta-specific habitat classes and emphasizes the high level of heterogeneity across
507 the delta. We compared the Lena Delta habitat classification to existing classifications: the first
508 published Lena Delta-wide land cover classification targeted towards tundra environments and the
509 upscaling of methane emissions with 30 m resolution (Schneider et al., 2009), the global ESA
510 Climate Change Initiative CCI land cover classification with 300 m resolution (Defourny, 2019), and a
511 circum-arctic standardized ESA GlobPermafrost land cover map of the Lena Delta with 20 m
512 resolution (Bartsch et al., 2019). We sampled the classification results with a regular point grid of
513 more than 3 million points which have an equal distance of 100 m to one another to compare the
514 classification results. Figures and tables with more information on class comparisons can be found in

the supplements (Table 1, Figure S3-5). Overall, the classifications of the Lena Delta overlap well for 'water' (water bodies (Defourny, 2019), shallow water (Schneider et al., 2009), water (different depths and sediment yields, Bartsch et al. 2019)) and 'sand' (bare areas (Defourny, 2019), mainly non-vegetated areas (Schneider et al., 2009), sand, seasonally inundated and disturbed (Bartsch et al. 2019)) areas. Besides this, the mapped classes differ greatly from one another. For example, the dominant classes in the coarse ESA CCI land cover 2018 product (300 m) for the Lena Delta are 'shrub or herbaceous cover', 'flooded', 'fresh / saline / brackish water', 'sparse vegetation (tree, shrub, herbaceous cover) (<15%)', and 'mosaic tree and shrub (>50%)', 'herbaceous cover (>50%)'.

These broad classes describe the major land cover in the Arctic delta but fail to depict the heterogeneity of habitats and plant communities not only because of its coarse spatial resolution but also because of the broad class descriptions. Furthermore, smaller areas are classified as 'tree cover', 'needleleaved', 'evergreen / deciduous', 'closed to open (>15%)' and 'mosaic tree and shrub (>50%) / herbaceous cover (<50%)' which is an inaccurate depiction of the delta.

This habitat map and the land cover classification from Schneider et al. (2009) resemble each other more closely, however, this habitat map shows more differentiation in the classes and spatial resolution, 10 m to 30 m, respectively. The only class description that is identical in both classifications, besides water and sand / mainly non-vegetated areas, is 'dry tussock tundra'. However, there is only a small match between these classes in the point comparison and most 'dry tussock tundra' areas from the Schneider et al. (2009) classification fall into the PC_50%, PC_20%, 'moist wet sedge complex' and 'dwarf shrub-herb communities'. The habitat map shows the mosaic of habitats on the floodplain with 'moist equisetum and shrubs on floodplain', 'dry low shrub community', 'moist to wet sedge' and 'wet sedge complex' which match with 'moist to dry dwarf shrub-dominated tundra' in the land cover classification of Schneider et al. (2009). Also, for the polygonal tundra complex, our habitat map shows more differentiation with three classes of up to 50% 20% 10% surface water contribution versus two classes in Schneider et al. (2009) 'wet sedge and moss dominated tundra' and 'moist grass and moss dominated tundra'. The areas covered by 'PC_50%' and 'PC_20%' match with 'wet sedge- and moss-dominated tundra', and 'PC_20%' and 'PC_10%' match with 'moist grass and moss-dominated tundra'. The overall aim of both maps is to differentiate between dry to wet land cover habitats as these describe the heterogeneity in the delta well and determine factors related to methane emissions (see Schneider et al. 2009) and the different habitat classes.

The land cover classification from ESA GlobPermafrost differentiates between 21 classes which are associated to eight broader groups, such as sparse vegetation, shrub tundra, forest, grassland, floodplain, disturbed, barren and water (Bartsch et al., 2019). With a spatial resolution of 20 m, the

Deleted: , S4m, S5

550 latter product is the closest to this habitat map. The major class 'wet ecotopes' of ESA
551 GlobPermafrost match with our 'PC_50%' on the first terrace and the 'moist to wet sedge complex'
552 on the floodplains. On the floodplain however, other classes show less agreement. The ESA
553 GlobPermafrost one class 'floodplain mostly fluvial' does not differentiate the floodplain classes
554 further, in contrast to our habitat map differentiating between 'moist to wet sedge complex', 'wet
555 sedge complex', 'moist equisetum and shrubs' and 'dry low shrub community' on floodplain.
556 Whereas the ESA GlobPermafrost class 'disturbed' (defined as forest fire scars, seasonally
557 inundation and landslide scars can be found in 'PC_50%' predominantly, in 'sand', 'PC_20%' and
558 'sparsely vegetated areas' in our habitat map. This underlines the complex structure of match and
559 mismatch between classifications.

560 The land cover map from Schneider et al. (2009) is based on two cloud-free Landsat images from
561 June/July 2000 and 2001, the ESA CCI land cover 2018 map is based on summer images as well.
562 Hence, the images used for this habitat classification were acquired at a similar time as for the ESA
563 CCI product and we do not expect differences based on changes on the ground due to this temporal
564 concurrence. In the almost 20-year difference between Schneider et al. (2009) and this habitat map
565 we do expect changes in vegetation composition. Overall, it is challenging to obtain sufficient cloud-
566 free images during the summer months to fully cover the entire Lena Delta for a classification project
567 and to depict a specific phenological state. Therefore, we created a Sentinel-2 composite mosaic
568 based on the maximum NDVI value per pixel from June to September. With this we ensure to have
569 the peak vegetation and phenology season represented as input for the habitat classification as
570 much as possible and increase comparability to other classification studies despite a temporal
571 mismatch.

572 The habitat map gives an accurate and detailed description of the Arctic Lena Delta that
573 incorporates extensive field data and expert knowledge. The habitat map is superior to the ESA CCI
574 land cover map (2018) in both spatial resolution and class description as it depicts the
575 heterogeneous habitat distribution. The 20m ESA GlobPermafrost classification matches the
576 resolution of the habitat map closely but due to its wider geographical application with circum-Arctic
577 standardized classes it does not optimally represent Lena Delta-specific habitats, such as the widely
578 distributed polygonal tundra complex. Furthermore, the habitat map is an update to Schneider et al.
579 (2009), which was based on three Landsat images from 2000 and 2001 and shows further
580 differentiation of habitats, specifically representing the floodplain mosaics of this Arctic delta.

581 4.3 Habitat linked disturbance regimes

Deleted: Note, that the lack of independent validation plots/pixels across the Lena Delta limits our ability to formally assess overall accuracy. This limitation might especially affect the smaller patchy habitat types, rather than the dominant types within the three terraces (see also visual evaluation in Figures S6-S8).

588 Parts of the Lena Delta are characterised by disturbances due to annual floodings or rapid
589 permafrost thaw processes leading to specific habitat classes. We provide habitat linked disturbance
590 regimes (describing the type and intensity of disturbances) across the delta. Our product (Dataset 6,
591 Figure 6a) shows that the largest part of the vegetated delta (excluding 12 439 km² of 'sand' and
592 'water' classes) is impacted by low disturbance, resulting in mature-state plant communities on the
593 terrace plateaus (Figure 6b, 72%, 12 806 km²). Specifically, the second terrace in the northwest of
594 the delta, with low ice content, is least impacted by rapid thaw processes and not part of the active
595 delta. In contrast, the habitats in the active delta are all linked to high disturbance (27%, 4 875 km²).
596 The 'moist to wet sedge complex' (10% of the vegetated Lena Delta) is the largest class considered
597 to be formed by high disturbance. This class is found in larger patch sizes on the riverine floodplains,
598 smaller patches on the floor of thermo-erosional valleys. Overall, 27.5% of the vegetated area of the
599 Lena Delta experiences some level of high disturbance from either regular spring floods or from
600 rapid thaw processes.

601 Species richness, relative abundance and biomass characteristics are important habitat features that
602 are influenced by landscape characteristics such as topography, water fluxes, soil types and
603 disturbance regimes (Forman and Godron, 1981; Naiman et al., 1986; Pickett et al., 1989;
604 Montgomery, 1999). Greig-Smith (1964), Woodwell and Whittaker (1968), and Forman and Godron
605 (1981) described fragmentation of land surfaces due to disturbance (defined by type and intensities)
606 and topography. In the Lena Delta, the terrace-related topography and active floodplain areas are
607 major determinants of plant communities and habitat classes and are thus well reflected in the Lena
608 Delta habitat map.

609 The high disturbance regime on floodplains results in 'shifting habitats' (Stanford et al., 2005; Driscoll
610 and Hauer, 2019). The annual spring floods and rapid thaw processes result in areas of high
611 disturbances, habitats of mid to advanced plant successional stages showing high vascular plant
612 above ground biomass (Figure 6c) due to the higher nutrient availability, a deeper active layer and
613 more moisture (e.g., Myers-Smith et al., 2020). Within the low disturbance habitat classes, a thick
614 moss layer as well as a low vascular plant coverage characterise the tundra community
615 assemblages representing mature state plant communities. Because high disturbance patches are
616 characterized by high vascular biomass, they can be well classified specifically in the NDVI, but also
617 NIR and red edge bands of optical medium resolution sensors such as SENTINEL-2. Within the
618 vegetation plots (Dataset 1), we did not find clear differences in species richness and in the Shannon
619 diversity index between the disturbed and the undisturbed classes (Figure 6d). Since most disturbed
620 habitat classes such as the 'moist to wet sedge', the 'wet sedge' as well as homogeneous patches of
621 high shrubs (as part of the habitat class 'dry grass to wet sedge complex'), were not sampled in the

622 field due to too challenging conditions, however they are clearly representing habitats with low
623 species richness. In the extreme case disturbance can lead to barren and sparsely vegetated
624 surfaces.

625 4.4 Classification accuracy and representativeness

626 The field data was acquired during a field trip in July-August 2018, primarily focusing on 30 m x 30 m
627 homogeneous vegetation and land cover plots. Additionally, we relied on Sentinel-2 images for the
628 different classifications that were also acquired in summer 2018, covering the same period as the
629 field trip, and have a spatial resolution of 20 m. The temporal overlap of the field work and the
630 satellite image acquisitions ensures consistency across the different datasets and represents a close
631 relationship between datasets and products obtained in the field (dataset 1, 2 and 3) and the results
632 derived from the satellite images that use the field data as input. As Sentinel-2 images have a small
633 geolocation error, we could link our field plot locations directly with the satellite images. Furthermore,
634 the sampling and measurement design of the plots with 30 m x 30 m ensured a reliable link to the
635 satellite data with similar spatial resolution, as we followed the recommendations on ESU. The
636 RGBNIR Sentinel-2 bands have a spatial resolution of 10 m and the red edge (NIR) and SWIR
637 bands a spatial resolution of 20 m, and even if we downsampled the bands to 10 m the spectral
638 information is sustained. More information on datasets and their spatial and temporal resolutions are
639 provided in supplementary Table S3.

640 The presented datasets are limited by the regional in-situ observations and expert knowledge
641 collected mainly in the central Lena Delta. The remoteness of the area and extremely difficult
642 logistics to conduct research in the second terrace and the outer rims of the delta are major reasons
643 for these limitations. However, the delta is relatively homogeneous in habitat classes that develop
644 based on underlying geomorphology and the disturbance regime (annual flooding and permafrost
645 thaw processes). Only one major habitat class is absent from the well studied central Lena Delta and
646 only occurs across the second terrace. For a formal evaluation of both habitat classification
647 products, we defined an independent test dataset within the central Lena Delta. The comparisons
648 show a relatively high accuracy for the central Lena Delta (94%) and a lower accuracy for the entire
649 Lena Delta classification (85%). While this decrease in accuracy was expected, due to the large
650 spatial extent of the Lena Delta, the limitation of independent evaluation restricted to the central
651 Lena Delta should be noted. Particularly for the smaller patchy habitat types the accuracy is likely
652 overestimated. For the large-scale patterns and the dominant habitat types, we are confident that the
653 classification results are reliable and accurate (see also visual evaluation in Figures S7-S9).

Deleted: Thus, even though detailed knowledge and in-situ observations are derived from a relatively small subset of the Delta, we are confident that our mapping results from the entire region are valuable and accurate. Also due to the inaccessibility of large areas of the delta, quantitative accuracy assessments of the classifier and the final mapping product are lacking. We had to rely on qualitative evaluation procedures by experts. Analysis of similarity of habitat classes and SENTINEL-2 spectral reflectance as well as NDVI values provide additional quantitative and qualitative assessments on the extent to which the different classes are identifiable and separated between classes.

667 In-situ observations (Datasets 1-3) as well as mapping products (Datasets 4-6) represent conditions
668 and vegetation composition of 2018. The timing of the summer 2018 expedition coincided with a
669 relatively high number of cloud free Sentinel-2 images necessary for a high quality habitat
670 classification. Overall, the described datasets are of appropriate quality to serve as a basis for
671 additional studies and most importantly as a baseline to identify changes in the future.

672 5 Conclusions

673 The described datasets provide coherent and complementary information of the major habitat
674 classes in the Lena Delta in Arctic Siberia, the largest delta in the Arctic. Based on extensive
675 knowledge collected during fieldwork that included habitat-related measurements of plant
676 composition, biomass, and hyperspectral field measurements we provide a validated and high-
677 resolution habitat classification map of the delta. In addition, we linked ecologically important
678 characteristics of disturbances in the delta to habitat classes, providing a baseline for future studies
679 of Arctic change as well as a foundation for potential upscaling of related processes such as
680 biodiversity, ecosystem functions, and biochemical dynamics such as greenhouse gas emissions.
681 With this update of previous land cover and habitat-related mapping products of the Lena Delta we
682 strive to facilitate and promote future investigations leading to a better understanding of this highly
683 sensitive arctic delta system.

684 Acknowledgements

685 Field work in the Lena River Delta was conducted in the frame of the Russian-German LENA
686 Expeditions based at Research Station Samoylov Island. We thank all colleagues and station staff
687 involved in the organization and logistics for their great support.

688 Code/Data availability

689 Dataset 1: Shevtsova et al., 2021a, <https://doi.pangaea.de/10.1594/PANGAEA.935875>, Foliage
690 projective cover of 26 vegetation sites in the central Lena Delta from 2018, is published as Foliage
691 projective cover for all major taxa estimated as percent, as tab-delimited text files.

692 Dataset 2: Shevtsova et al., 2021b, <https://doi.pangaea.de/10.1594/PANGAEA.935923>, Total above-
693 ground biomass of 25 vegetation sites in the central Lena Delta from 2018, is published as biomass

694 aboveground dry mass per major taxa, as well as for 'moss and lichen', 'litter' and the remaining minor
695 taxa (called 'other plants') and the total biomass in the units [g/m²], as tab-delimited text.

696 Dataset 3: Runge et al., 2022, <https://doi.pangaea.de/10.1594/PANGAEA.945982>, Hyperspectral field
697 spectrometry of Arctic vegetation units in the central Lena Delta, is published as an overview of the
698 plot details and field spectrometer reflectance spectra in the unit [%] of 28 vegetation plots, as tab-
699 delimited text files.

700 Dataset 4: Landgraf et al., 2022 a,b,c. The Sentinel-2-derived central Lena Delta land cover (habitat)
701 classification consists of the following three data publications: i) Landgraf et al. 2022a,
702 <https://doi.pangaea.de/10.1594/PANGAEA.945056>: a raster file with assigned land cover classes and an
703 ESRI polygon shape file containing the 10 training classes representing the different vegetation
704 compositions, as geotiff file. Both datasets are based on 2018 satellite images and informed by the in-situ
705 vegetation plots and expert knowledge. Datasets are in Universe Transverse Mercator (UTM) Zone 52
706 North projection. ii) Landgraf et al. 2022b, <https://doi.pangaea.de/10.1594/PANGAEA.945054>. This data
707 set includes training elements representing different vegetation composition in the form of Elementary
708 Sampling Units ESUs: 69 pseudo ESUs set with expert knowledge from the field and from Lena Delta
709 expedition field reports. iii) Landgraf et al. 2022c, <https://doi.pangaea.de/10.1594/PANGAEA.945055>.
710 This data set includes training elements representing different vegetation composition in the form of
711 Elementary Sampling Units ESUs: 23 true ESUs representing the LD18 vegetation plots.

712 Dataset 5: Lisovski et al., 2022, <https://doi.pangaea.de/10.1594/PANGAEA.946407>. The Lena Delta
713 Habitat Map (2018, Sentinel-2) contains i) the Lena Delta habitat map (13 classes), ii) the sand probability
714 map, both as geotiff files in WGS84 geographic projection, iii) the habitat class description as comma
715 delimited csv table, and iv) the training dataset (n = 4 278 classified pixels) in geographic decimal
716 coordinates comma delimited csv table. The data collection also contains the Lena Delta Region of
717 Interest (ROI) ESRI shapefile outlining the Lena Delta including a coastal water buffer.

718 Dataset 6: Heim and Lisovski, 2023, <https://doi.org/10.5281/zenodo.7575691>. The Lena Delta habitat
719 disturbance regime map is published in the form of two geotiff files (tiles) in WGS84 geographic
720 projection.

721 Code developed in Google Earth Engine to derive habitat classes based in the central Lena Delta
722 classification, as well as R code for figures can be accessed from the following repository: Lisovski,
723 S. (2024). Code for 'A new habitat map of the Lena Delta in Arctic Siberia based on field and remote
724 sensing datasets'. V0.1. Zenodo. 10.5281/zenodo.11197641.

725 Competing interests

726 Birgit Heim is a member of the editorial board of ESSD. Otherwise, we declare no competing interests.

727 Funding

728 SL acknowledges funding from the Geo.X Network for Geosciences in Berlin and Brandenburg. This
729 study was supported by BMBF KoPf (Grant Number 03F0764B), KoPf Synthesis (Grant Number
730 03F0834B), and AWI base funds. AR was partially funded by ESA GlobPermafrost and an ESA CCI
731 postdoctoral fellowship. BH acknowledges HGF REKLIM.

732 Authors contribution

733 SL: Conceptual framework, habitat classification, data analysis, writing

734 AR: Conceptual framework, field work, spectral field data collection, habitat classification, spectral
735 data processing, data analysis, writing

736 IS: Field work, biomass and projective cover measurement in vegetation plots, habitat classification

737 RRO: Habitat classification

738 NL: habitat classification, spectral data processing

739 MF: Field work, spectral field data collection

740 NiL: habitat class definition, field work

741 AM: Project management, writing

742 CS: Spectral data processing

743 AB: Spectral data processing

744 UH: Conceptual framework, project management

745 GG: Conceptual framework, project management, habitat classification, writing

746 BH: Conceptual framework, field work, habitat classification, project management, writing

748

749

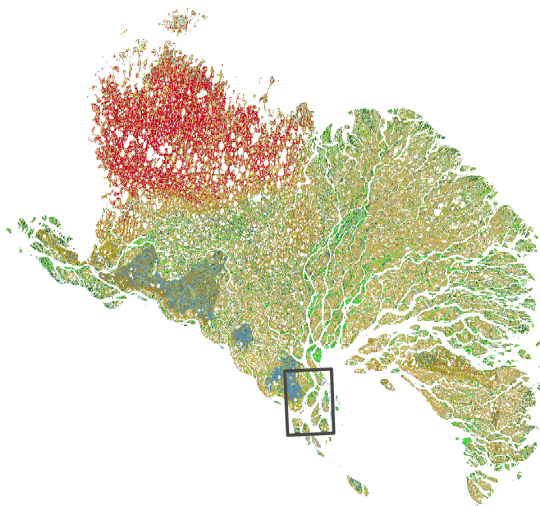


Figure A1: Location of the central Lena Delta *habitat classification* (Dataset 4) in the Lena Delta (Dataset 5,6).

750

754

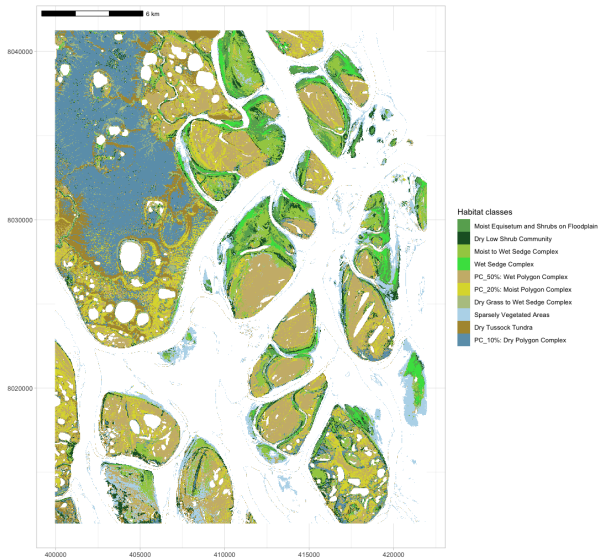
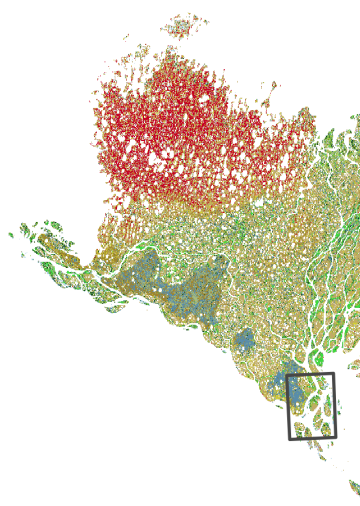


Figure A2: Supervised habitat classification of the central Lena Delta based on a cloud-free Sentinel-2 August 2018 acquisition (Dataset 4). Numbers in legend correspond to the labels in published Dataset 4 (Landgraf et al. 2022).

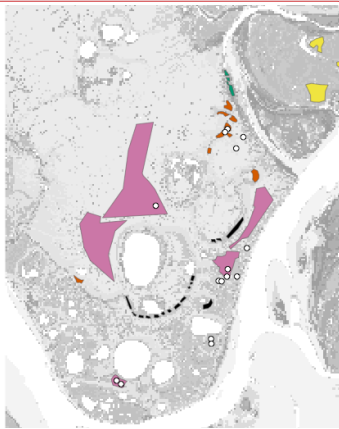


Deleted:

Deleted: WGS 84 projection.

Deleted: <object>

Deleted: Universe Transverse Mercator Z52 on WGS 84 projection.



Deleted:

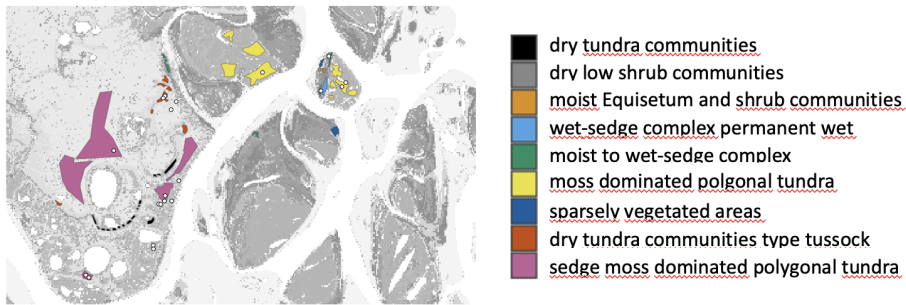


Figure A3: The central Lena Delta with 30 x 30 m ESUs (white points, dataset 1) and polygonal shapefiles defined by expert knowledge (published with dataset 4). Together the ESUs and polygonal shapefiles served areas to sample 8 626 training pixels for the central Lena Delta landcover/habitat classification (dataset 4, Landgraf et al. 2022a).

Deleted: Subset of

Deleted: polygons

Deleted: polygons

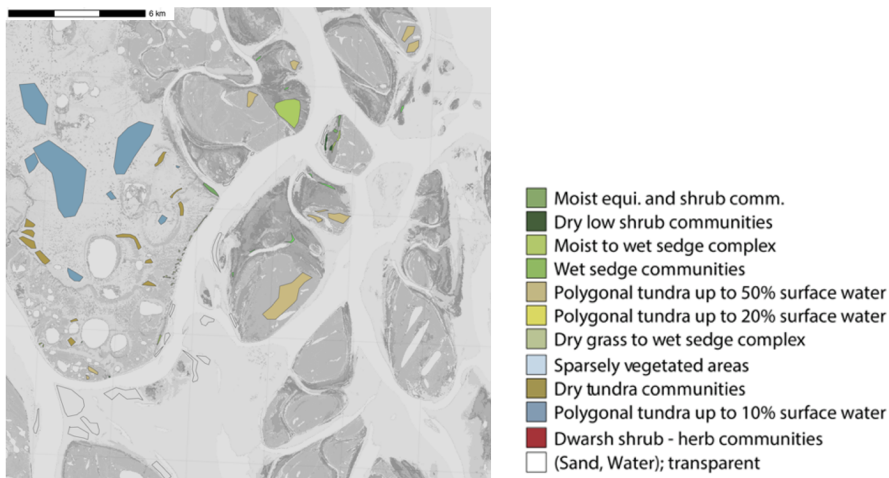


Figure A4: Central Lena Delta with the additionally defined polygonal shapefiles as a test dataset for independent evaluation. The polygonal shapefiles were defined using high resolution satellite and drone images, and extensive knowledge from the field (Heim et al. 2025).

Deleted: Table A1: Results of the class-based cross-validation for the central Lena Delta habitat classification, based in 50 % of the 8 626 labelled pixels, and the accuracy of the classifier (e.g., resubstitution error) of the entire Lena Delta habitat classifier.

Table A1: Confusion matrix and statistics of the central Lena Delta habitat classification with independently defined polygons (Figure A4, Heim et al. 2025). Statistics are based on 100 random samples per class (1 100 samples). Classes refer to 0 = Moist equi. and shrub community, 1 = Dry low shrub community, 2 =Moist wet sedge community, 3 = Wet sedge community, 4 = Polygonal tundra (50%), 6 =Dry grass and wet sedge complex, 8 = Dry tundra communities, 9 = Polygonal tundra, 10 = Sand.

Overall Statistics:										
Accuracy	0.94									
95% CI	(0.9223 – 0.9548)									
No Information Rate	0.1199									
P-Value [Acc > NIR]	< 2.2e-16									
Kappa	0.9325									
Class	0	1	2	3	4	6	8	9	10	
Sensitivity	0.89	0.93	0.87	0.88	0.96	0.92	0.98	0.98	1.00	
	53	00	74	35	97	78	99	94	00	
Specificity	0.97	0.99	0.99	0.98	0.99	0.98	0.99	0.99	1.00	
	74	87	49	85	75	73	75	11	00	
Pos Pred	0.81	0.98	0.95	0.91	0.97	0.90	0.98	0.93	1.00	
	05	94	88	00	96	00	00	00	00	
Neg Pred	0.98	0.99	0.98	0.98	0.99	0.99	0.99	0.99	1.00	
	86	11	35	47	62	11	87	87	00	
Prevalence	0.81	0.98	0.95	0.91	0.97	0.90	0.98	0.93	1.00	
	05	94	88	00	96	00	00	00	00	
Detection Rate	0.89	0.93	0.87	0.88	0.96	0.92	0.98	0.98	1.00	
	53	00	74	35	97	78	99	94	00	
Detection Prevalence	0.85	0.95	0.91	0.89	0.97	0.91	0.98	0.95	1.00	
	08	88	63	66	46	37	49	88	00	
Balanced Accuracy	0.09	0.11	0.11	0.11	0.11	0.10	0.11	0.10	0.11	
	73	31	99	65	20	97	20	63	31	

Table A2: Confusion matrix and statistics of the entire Lena Delta habitat classification with independently defined polygons (Figure A5). Note, that polygons are from the central Lena Delta only and evaluation statistics are only representative for a small spatial subset of the entire Lena Delta. Statistics are based on 100 random samples per class (1 100 samples). Classes refer to 0 = Moist equisetum and shrub community, 1 = Dry low shrub community, 2 =Moist wet sedge community, 3 = Wet sedge community, 4 = Polygonal tundra (50%), 6 =Dry grass and wet sedge complex, 8 = Dry tundra communities, 9 = Polygonal tundra.

Overall Statistics:									
Accuracy	0.8431								
95% CI	(0.8157 – 0.8679)								
No Information Rate	0.1722								
P-Value [Acc > NIR]	< 2.2e-16								
Kappa	0.8207								
Class	0	1	2	3	4	6	8	9	
Sensitivity	0.742	0.932	0.689	0.702	0.912	0.956	1.000	0.960	
Specificity	0.957	0.961	0.989	0.980	0.999	0.951	0.991	0.996	
Pos Pred	0.688	0.708	0.930	0.870	0.989	0.650	0.939	0.970	
Neg Pred	0.967	0.993	0.939	0.946	0.987	0.996	1.000	0.994	
Prevalence	0.688	0.708	0.930	0.870	0.989	0.650	0.939	0.970	

Deleted: Habitat class
Deleted Cells ... [11]
Deleted: Abbreviation
Deleted Cells ... [21]
Deleted: – central Lena Delta
Inserted Cells ... [31]
Inserted Cells ... [41]
Inserted Cells ... [51]
Inserted Cells ... [61]
Inserted Cells ... [71]
Inserted Cells ... [81]
Inserted Cells ... [91]
Deleted: Accuracy – entire Lena Delta
Deleted: Moist equisetum and shrub community
Deleted: MESH
Deleted: 999
Deleted: 0.977
Deleted Cells ... [101]
Deleted: Dry shrub community
Deleted: DSH
Deleted: 0.947
Deleted: 998
Deleted: Moist to wet sedge community
Deleted: 0.997
Deleted: 0.972
Deleted: MSWS
Deleted: Wet sedge community
Deleted: WS
Deleted: 0.947
Deleted Cells ... [111]
Inserted Cells ... [121]
Deleted: 991
Deleted: Polygonal tundra (up to 50% surface water)
Deleted: PC < 50%
Deleted: .988
Deleted: 0.978
Inserted Cells ... [131]
Deleted: Polygonal tundra (up to 20% surface water)
Deleted: PC < 20%
Deleted: 986
Deleted: 925
Deleted: Dry grass to wet sedge community
Deleted: GSSH
Deleted: 990
Deleted: 918
Deleted: Sparsely vegetated area
Deleted: SPSH
Deleted: 999
Deleted: 948
Deleted: Dry tundra (tussock tundra)
Deleted: DT
Deleted: 993
Deleted: 94
Deleted: Polygonal tundra (up to 10% surface water)
Deleted: PC<10%
Deleted: 996
Deleted: 985
Deleted: Dwarf shrub-herb community
Deleted: DSC

<i>Detection Rate</i>	<u>0.742</u>	<u>0.932</u>	<u>0.689</u>	<u>0.702</u>	<u>0.912</u>	<u>0.956</u>	<u>1.000</u>	<u>0.960</u>
<i>Detection Prevalence</i>	<u>0.714</u>	<u>0.805</u>	<u>0.791</u>	<u>0.777</u>	<u>0.949</u>	<u>0.774</u>	<u>0.969</u>	<u>0.965</u>
<i>Balanced Accuracy</i>	<u>0.114</u>	<u>0.093</u>	<u>0.172</u>	<u>0.158</u>	<u>0.130</u>	<u>0.087</u>	<u>0.119</u>	<u>0.128</u>

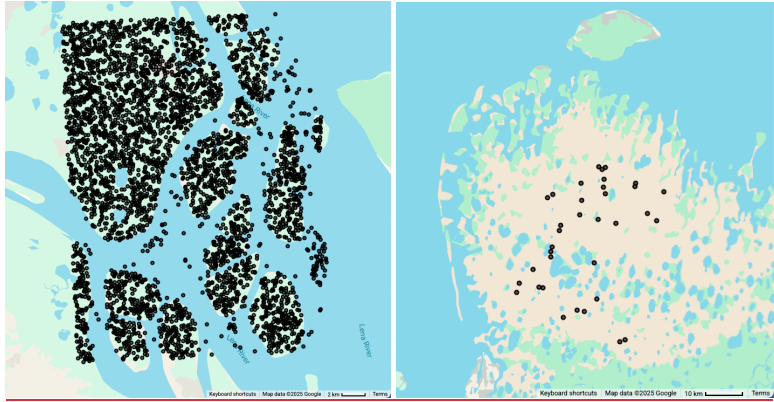


Figure A4: Training pixels for the Lena Delta habitat classification (dataset 5). (Left) 7,500 random ~~pixel~~ samples across the habitat classes from the central Lena Delta landcover/habitat map (dataset 4). (Right) 35 pixels (ESUS, Landgraf et al. 2022) selected by expert knowledge for the 'dwarf shrub - herb communities' that are missing in the central Lena Delta.

Deleted: pixels

926 References

927 AMAP: AMAP Arctic Climate Change Update 2021: Key Trends and Impacts. Arctic Monitoring
928 and Assessment Programme (AMAP), Tromsø, Norway, viii+148pp, 2021.

929 Bartlett, K. B., Crill, P. M., Sass, R. L., Harriss, R. C., and Dise, N. B.: Methane Emissions from
930 Tundra Environments in the Yukon-Kuskokwim Delta, Alaska, Journal of Geophysical
931 Research-Atmospheres, 97, 16645-16660, <https://doi.org/10.1029/91jd00610>, 1992.

Deleted: :

932 Bartsch, A., Hofer, A., Kroisleitner, C., and Trofai, A. M.: Land Cover Mapping in Northern
933 High Latitude Permafrost Regions with Satellite Data: Achievements and Remaining
934 Challenges, Remote Sensing, 8, 979, <https://doi.org/10.3390/rs8120979>, 2016.

Deleted: :

935 Bartsch, A., Widhalm, B., Pointner, G., Ermokhina, K., Leibman, M., and Heim, B.: Landcover
936 derived from Sentinel-1 and Sentinel-2 satellite data (2015-2018) for subarctic and arctic
937 environments [dataset], <https://doi.org/10.1594/PANGAEA.897916>, 2019.

938 Bartsch, A., Widhalm, B., Leibman, M., Ermokhina, K., Kumpula, T., Skarin, A., Wilcox, E. J.,
939 Jones, B. M., Frost, G. V., Hofer, A., and Pointner, G.: Feasibility of tundra vegetation height
940 retrieval from Sentinel-1 and Sentinel-2 data, Remote Sensing of Environment, 237, 111515,
941 <https://doi.org/10.1016/j.rse.2019.111515>, 2020.

Deleted: :

942 Beamish, A., Reynolds, M. K., Epstein, H., Frost, G. V., Macander, M. J., Bergstedt, H., Bartsch,
943 A., Kruse, S., Miles, V., Tanis, C. M., Heim, B., Fuchs, M., Chabrilat, S., Shevtsova, I.,
944 Verdonen, M., and Wagner, J.: Recent trends and remaining challenges for optical remote
945 sensing of Arctic tundra vegetation: A review and outlook, Remote Sensing of Environment,
946 246, ARTN 111872, <https://doi.org/10.1016/j.rse.2020.111872>, 2020.

Deleted: :

947 Beamish, A. L., Coops, N., Chabrilat, S., and Heim, B.: A Phenological Approach to Spectral
948 Differentiation of Low-Arctic Tundra Vegetation Communities, North Slope, Alaska, Remote
949 Sensing, 9, 1200, <https://doi.org/10.3390/rs9111200>, 2017.

Deleted: :

950 Beamish, A. L., Coops, N. C., Hermosilla, T., Chabrilat, S., and Heim, B.: Monitoring pigment-
951 driven vegetation changes in a low-Arctic tundra ecosystem using digital cameras, Ecosphere,
952 9, e02123, <https://doi.org/10.1002/ecs2.2123>, 2018.

Deleted: :

959 Berner, L. T., Massey, R., Jantz, P., Forbes, B. C., Macias-Fauria, M., Myers-Smith, I.,
960 Kumpula, T., Gauthier, G., Andreu-Hayles, L., Gaglioti, B. V., Burns, P., Zetterberg, P., D'Arrigo,
961 R., and Goetz, S. J.: Summer warming explains widespread but not uniform greening in the
962 Arctic tundra biome, *Nature Communications*, 11, 4621, [https://doi.org/10.1038/s41467-020-](https://doi.org/10.1038/s41467-020-18479-5)
963 18479-5, 2020.

Deleted: :

964 Biskaborn, B. K., Smith, S. L., Noetzli, J., Matthes, H., Vieira, G., Streletskiy, D. A., Schoeneich,
965 P., Romanovsky, V. E., Lewkowicz, A. G., Abramov, A., Allard, M., Boike, J., Cable, W. L.,
966 Christiansen, H. H., Delaloye, R., Diekmann, B., Drozdov, D., Etzelmuller, B., Grosse, G.,
967 Guglielmin, M., Ingeman-Nielsen, T., Isaksen, K., Ishikawa, M., Johansson, M., Johannsson, H.,
968 Joo, A., Kaverin, D., Kholodov, A., Konstantinov, P., Kroger, T., Lambiel, C., Lanckman, J. P.,
969 Luo, D. L., Malkova, G., Meiklejohn, I., Moskalenko, N., Oliva, M., Phillips, M., Ramos, M.,
970 Sannel, A. B. K., Sergeev, D., Seybold, C., Skryabin, P., Vasiliev, A., Wu, Q. B., Yoshikawa, K.,
971 Zheleznyak, M., and Lantuit, H.: Permafrost is warming at a global scale, *Nature*
972 *Communications*, 10, 264, <https://doi.org/10.1038/s41467-018-08240-4>, 2019.

Deleted: :

973 Boike, J., Wille, C., and Abnizova, A.: Climatology and summer energy and water balance of
974 polygonal tundra in the Lena River Delta, Siberia, *Journal of Geophysical Research-*
975 *Biogeosciences*, 113, G03025, <https://doi.org/10.1029/2007jg000540>, 2008.

Deleted: :

976 Boike, J., Nitzbon, J., Anders, K., Grigoriev, M., Bolshiyarov, D., Langer, M., Lange, S.,
977 Bornemann, N., Morgenstern, A., Schreiber, P., Wille, C., Chadburn, S., Gouttevin, I., Burke, E.,
978 and Kutzbach, L.: A 16-year record (2002-2017) of permafrost, active-layer, and meteorological
979 conditions at the Samoylov Island Arctic permafrost research site, Lena River delta, northern
980 Siberia: an opportunity to validate remote-sensing data and land surface, snow, and permafrost
981 models, *Earth System Science Data*, 11, 261-299, <https://doi.org/10.5194/essd-11-261-2019>,
982 2019.

Deleted: :

983 Box, J. E., Colgan, W. T., Christensen, T. R., Schmidt, N. M., Lund, M., Parmentier, F. J. W.,
984 Brown, R., Bhatt, U. S., Euskirchen, E. S., Romanovsky, V. E., Walsh, J. E., Overland, J. E.,
985 Wang, M. Y., Corell, R. W., Meier, W. N., Wouters, B., Mernild, S., Mard, J., Pawlak, J., and
986 Olsen, M. S.: Key indicators of Arctic climate change: 1971-2017, *Environmental Research*
987 *Letters*, 14, 045010, <https://doi.org/10.1088/1748-9326/aafc1b>, 2019.

Deleted: :

988 Buchhorn, M., Walker, D. A., Heim, B., Reynolds, M. K., Epstein, H. E., and Schwieder, M.:
989 Ground-Based Hyperspectral Characterization of Alaska Tundra Vegetation along

995 Environmental Gradients, Remote Sensing, 5, 3971-4005, <https://doi.org/10.3390/rs5083971>,
996 2013.

Deleted: :

997 Driscoll, K. P. and Hauer, F. R.: Seasonal flooding affects habitat and landscape dynamics of a
998 gravel-bed river floodplain, Freshwater Science, 38, 510-526, <https://doi.org/10.1086/704826>,
999 2019.

Deleted: :

1000 Drusch, M., Del Bello, U., Carlier, S., Colin, O., Fernandez, V., Gascon, F., Hoersch, B., Isola,
1001 C., Laberinti, P., Martimort, P., Meygret, A., Spoto, F., Sy, O., Marchese, F., Bargellini, P.,
1002 Sentinel-2: ESA's optical high-resolution mission for GMES operational services. Rem. Sens.
1003 Environ., 120, 25-36, <https://doi.org/10.1016/j.rse.2011.11.026>, 2012.

Deleted: :

1004 Duncanson, L., Armston, J., Disney, M., Avitabile, V., Barbier, N., Calders, K., Carter, S.,
1005 Chave, J., Herold, M., MacBean, N., McRoberts, R., Minor, D., Paul, K., Réjou-Méchain, M.,
1006 Roxburgh, S., Williams, M., Albinet, C., Baker, T., Bartholomeus, H., Bastin, J. F., Coomes, D.,
1007 Crowther, T., Davies, S., de Bruin, S., De Kauwe, M., Domke, G., Dubayah, R., Falkowski, M.,
1008 Fatoyinbo, L., Goetz, S., Jantz, P., Jonckheere, I., Jucker, T., Kay, H., Kellner, J., Labriere, N.,
1009 Lucas, R., Mitchard, E., Morsdorf, F., Næsset, E., Park, T., Phillips, O. L., Ploton, P., Puliti, S.,
1010 Quegan, S., Saatchi, S., Schaaf, C., Schepaschenko, D., Scipal, K., Stovall, A., Thiel, C.,
1011 Wulder, M. A., Camacho, F., Nickeson, J., Román, M., and Margolis, H.: Aboveground Woody
1012 Biomass Product Validation Good Practices Protocol. Version 1.0, Land Product Validation
1013 Subgroup (WGCV/CEOS), <https://doi.org/10.5067/doc/ceoswgcv/lpv/agb.001>, 2021.

Deleted: :

1014 Endsley, K. A., Kimball, J. S., and Reichle, R. H.: Soil Respiration Phenology Improves Modeled
1015 Phase of Terrestrial net Ecosystem Exchange in Northern Hemisphere, Journal of Advances in
1016 Modeling Earth Systems, 14, e2021MS002804, <https://doi.org/10.1029/2021MS002804>, 2022.

Deleted: :

1017 ESA, 2015. Sentinel-2 User Handbook. ESA Standard Document.

1018 ESA Land Cover CCI project team; Defourny, P. (2019): ESA Land Cover Climate Change
1019 Initiative (Land_Cover_cci): Global Land Cover Maps, Version 2.0.7. Centre for
1020 Environmental Data Analysis, *downloaded 2022*, [dataset]
1021 <https://catalogue.ceda.ac.uk/uuid/b382ebe6679d44b8b0e68ea4ef4b701c>

1022 Fedorova, I., Chetverova, A., Bolshiyarov, D., Makarov, A., Boike, J., Heim, B., Morgenstern,
1023 A., Overduin, P. P., Wegner, C., Kashina, V., Eulenburg, A., Dobrotina, E., and Sidorina, I.:

1029 Lena Delta hydrology and geochemistry: long-term hydrological data and recent field
1030 observations, *Biogeosciences*, 12, 345-363, <https://doi.org/10.5194/bg-12-345-2015>, 2015.

1031 Forman, R. T. T. and Godron, M.: Patches and Structural Components for a Landscape
1032 Ecology, *Bioscience*, 31, 733-740, <https://doi.org/10.2307/1308780>, 1981.

1033 Frost, G. V., Loehman, R. A., Saperstein, L. B., Macander, M. J., Nelson, P. R., Paradis, D. P.,
1034 and Natali, S. M.: Multi-decadal patterns of vegetation succession after tundra fire on the
1035 Yukon-Kuskokwim Delta, Alaska, *Environmental Research Letters*, 15, 025003,
1036 <https://doi.org/10.1088/1748-9326/ab5f49>, 2020.

1037 Gilg, O., Sané, R., Solovieva, D. V., Pozdnyakov, V. I., Sabard, B., Tsanos, D., Zöckler, C.,
1038 Lappo, E. G., Syroechkovski, J. E. E., and Eichhorn, G.: Birds and Mammals of the Lena Delta
1039 Nature Reserve, Siberia, *ARCTIC*, 53, 118-133, <https://doi.org/10.14430/arctic842>, 2000.

1040 Greig-Smith, P.: Quantitative plant ecology, Butterworths 1964.

1041 Grigoriev, M. N.: Crio Morphogenesis in the Lena Delta, Permafrost Institute Press, Yakutsk
1042 1993.

1043 Heim, B., Lisovski, S., & Runge, A.: Polygonal shapefiles as test dataset for the Central Lena
1044 Delta Classification (Landgraf et al. in review) [Data set]. [Zenodo](https://doi.org/10.5281/zenodo.14731823).
1045 <https://doi.org/10.5281/zenodo.14731823>, 2025

1046 Heim, B. and Lisovski, S.: Lena Delta habitat disturbance regimes (0.0) [dataset], [Zenodo](https://doi.org/10.5281/zenodo.7575691),
1047 <https://doi.org/10.5281/zenodo.7575691>, 2023.

1048 Holl, D., Wille, C., Sachs, T., Schreiber, P., Runkle, B. R. K., Beckebanze, L., Langer, M., Boike,
1049 J., Pfeiffer, E. M., Fedorova, I., Bolshianov, D. Y., Grigoriev, M. N., and Kutzbach, L.: A long-
1050 term (2002 to 2017) record of closed-path and open-path eddy covariance CO2 net ecosystem
1051 exchange fluxes from the Siberian Arctic, *Earth System Science Data*, 11, 221-240,
1052 <https://doi.org/10.5194/essd-11-221-2019>, 2019.

1053 Hu, F. S., Higuera, P. E., Duffy, P., Chipman, M. L., Rocha, A. V., Young, A. M., Kelly, R., and
1054 Dietze, M. C.: Arctic tundra fires: natural variability and responses to climate change, *Frontiers*
1055 *in Ecology and the Environment*, 13, 369-377, <https://doi.org/10.1890/150063>, 2015.

Deleted: :

Deleted: :

Deleted: :

Deleted: :

Deleted: :

1061 Hubberten, H.-W., Wagner, D., Pfeiffer, E.-M., Boike, J., and Gukov, A. Y.: The Russian-
 1062 German research station samoylov, Lena delta -A key site for polar research in the Siberian
 1063 arctic, Polarforschung, 2006.

1064 Jorgenson, M. T.: Hierarchial organisation of ecosystems at multiple spatial scales on the
 1065 Yukon-Kuskokwim Delta, Alaska, USA, Arctic Antarctic and Alpine Research, 32, 221-239,
 1066 <https://doi.org/10.2307/1552521>, 2000.

1067 Juhls, B., Antonova, S., Angelopoulos, M., Bobrov, N., Grigoriev, M., Langer, M., Maksimov, G.,
 1068 Miesner, F., and Overduin, P. P.: Serpentine (Floating) Ice Channels and their Interaction with
 1069 Riverbed Permafrost in the Lena River Delta, Russia, Frontiers in Earth Science, 9, 689941,
 1070 <https://doi.org/10.3389/feart.2021.689941>, 2021.

1071 Kienast, F. and Tsherkasova, J.: Comparative botanical recent-studies in the Lena River Delta
 1072 [Field Report], Alfred Wegener Institute, Germany, 2001.

1073 Landgraf, N., Shevtsova, I., Pflug, B., and Heim, B. .: Sentinel-2 derived central Lena Delta land
 1074 cover classification, PANGAEA [dataset], <https://doi.pangaea.de/10.1594/PANGAEA.945057>,
 1075 2022a.

1076 Landgraf, N., Shevtsova, I., Pflug, B., and Heim, B.: Raster file with assigned land cover classes
 1077 and ESRI polygon shape file training classes representing different vegetation composition,
 1078 PANGAEA [dataset], <https://doi.pangaea.de/10.1594/PANGAEA.945056>, 2022b.

1079 Landgraf, N., Shevtsova, I., Pflug, B., and Heim, B.: 23 true Elementary Sampling Units (ESUs)
 1080 set in the Lena Delta representing the LD18 vegetation plots, PANGAEA [dataset],
 1081 <https://doi.pangaea.de/10.1594/PANGAEA.945055>, 2022c.

1082 Landgraf, N., Shevtsova, I., Pflug, B., and Heim, B.: 69 pseudo Elementary Sampling Units
 1083 (ESUs) set in the Lena Delta derived with expert knowledge, PANGAEA [dataset],
 1084 <https://doi.pangaea.de/10.1594/PANGAEA.945054>, 2022d.

1085 Lantz, T. C., Kokelj, S. V., and Fraser, R. H.: Ecological recovery in an Arctic delta following
 1086 widespread saline incursion, Ecological Applications, 25, 172-185, <https://doi.org/10.1890/14-0239.1>, 2015.

Deleted: :

Deleted: :

1090 Lisovski, S., Runge, A., Okoth, R. R., Shevtsova, I., and Heim, B.: Lena Delta Land Cover
 1091 Classification (2018, Sentinel-2), PANGAEA [dataset],
 1092 <https://doi.org/10.1594/PANGAEA.946407>, 2022.
 1093 Lorang, M. S. and Hauer, F. R.: Fluvial geomorphic processes, in: Methods in stream ecology,
 1094 edited by: Hauer, F. R., and Lamberti, G. A., Academic Press/Elsevier, San Diego, 145–168,
 1095 2006.
 1096 Macander, M. J., Nelson, P. R., Nawrocki, T. W., Frost, G. V., Orndahl, K. M., Palm, E. C.,
 1097 Wells, A. F., and Goetz, S. J.: Time-series maps reveal widespread change in plant functional
 1098 type cover across Arctic and boreal Alaska and Yukon, Environmental Research Letters, 17,
 1099 ARTN 054042, <https://doi.org/10.1088/1748-9326/ac6965>, 2022.
 1100 Mauclet, E., Agnan, Y., Hirst, C., Monhonval, A., Pereira, B., Vandeuren, A., Villani, M.,
 1101 Ledman, J., Taylor, M., Jasinski, B. L., Schuur, E. A. G., and Opfergelt, S.: Changing sub-Arctic
 1102 tundra vegetation upon permafrost degradation: impact on foliar mineral element cycling,
 1103 Biogeosciences, 19, 2333-2351, <https://doi.org/10.5194/bg-19-2333-2022>, 2022.
 1104 Mekonnen, Z. A., Riley, W. J., Berner, L. T., Bouskill, N. J., Torn, M. S., Iwahana, G., Breen, A.
 1105 L., Myers-Smith, I. H., Criado, M. G., Liu, Y. L., Euskirchen, E. S., Goetz, S. J., Mack, M. C., and
 1106 Grant, R. F.: Arctic tundra shrubification: a review of mechanisms and impacts on ecosystem
 1107 carbon balance, Environmental Research Letters, 16, 053001, [https://doi.org/10.1088/1748-](https://doi.org/10.1088/1748-9326/abf28b)
 1108 9326/abf28b, 2021.
 1109 Montgomery, D. R.: Process domains and the river continuum, Journal of the American Water
 1110 Resources Association, 35, 397-410, <https://doi.org/10.1111/j.1752-1688.1999.tb03598.x>,
 1111 1999.
 1112 Morgenstern, A., Grosse, G., and Schirrmeister, L.: Genetic, morphological, and statistical
 1113 characterization of lakes in the permafrost-dominated Lena Delta, Ninth International
 1114 Conference on Permafrost, 2008.
 1115 Morgenstern, A., Grosse, G., Gunther, F., Fedorova, I., and Schirrmeister, L.: Spatial analyses
 1116 of thermokarst lakes and basins in Yedoma landscapes of the Lena Delta, Cryosphere, 5, 849-
 1117 867, <https://doi.org/10.5194/tc-5-849-2011>, 2011.

Deleted: :

Deleted: :

Deleted: :

Deleted: :

Deleted: :

Deleted: :

- 1124 Morgenstern, A., Overduin, P. P., Gunther, F., Stettner, S., Ramage, J., Schirrmeister, L.,
 1125 Grigoriev, M. N., and Grosse, G.: Thermo-erosional valleys in Siberian ice-rich permafrost,
 1126 Permafrost and Periglacial Processes, 32, 59-75, <https://doi.org/10.1002/ppp.2087>, 2021.
- 1127 Morgenstern, A., Ulrich, M., Gunther, F., Roessler, S., Fedorova, I. V., Rudaya, N. A., Wetterich,
 1128 S., Boike, J., and Schirrmeister, L.: Evolution of thermokarst in East Siberian ice-rich
 1129 permafrost: A case study, Geomorphology, 201, 363-379,
 1130 <https://doi.org/10.1016/j.geomorph.2013.07.011>, 2013.
- 1131 Mueller-Bombois, D. and Ellenberg, H.: Aims and methods of vegetation ecology, John Wiley &
 1132 Sons, New York, USA1974.
- 1133 Myers-Smith, I. H., Kerby, J. T., Phoenix, G. K., Bjerke, J. W., Epstein, H. E., Assmann, J. J.,
 1134 John, C., Andreu-Hayles, L., Angers-Blondin, S., Beck, P. S. A., Berner, L. T., Bhatt, U. S.,
 1135 Bjorkman, A. D., Blok, D., Bryn, A., Christiansen, C. T., Cornelissen, J. H. C., Cunliffe, A. M.,
 1136 Elmendorf, S. C., Forbes, B. C., Goetz, S. J., Hollister, R. D., de Jong, R., Lorant, M. M.,
 1137 Macias-Fauria, M., Maseyk, K., Normand, S., Olofsson, J., Parker, T. C., Parmentier, F. J. W.,
 1138 Post, E., Schaepman-Strub, G., Stordal, F., Sullivan, P. F., Thomas, H. J. D., Tommervik, H.,
 1139 Treharne, R., Tweedie, C. E., Walker, D. A., Wilmsking, M., and Wipf, S.: Complexity revealed in
 1140 the greening of the Arctic, Nature Climate Change, 10, 106-117,
 1141 <https://doi.org/10.1038/s41558-019-0688-1>, 2020.
- 1142 Naiman, R. J., Melillo, J. M., and Hobbie, J. E.: Ecosystem Alteration of Boreal Forest Streams
 1143 by Beaver (*Castor-Canadensis*), Ecology, 67, 1254-1269, <https://doi.org/10.2307/1938681>,
 1144 1986.
- 1145 Nitzbon, J., Westermann, S., Langer, M., Martin, L. C. P., Strauss, J., Laboor, S., and Boike, J.:
 1146 Fast response of cold ice-rich permafrost in northeast Siberia to a warming climate, Nature
 1147 Communications, 11, 2201, <https://doi.org/10.1038/s41467-020-15725-8>, 2020.
- 1148 Nitze, I. and Grosse, G.: Detection of landscape dynamics in the Arctic Lena Delta with
 1149 temporally dense Landsat time-series stacks, Remote Sensing of Environment, 181, 27-41,
 1150 <https://doi.org/10.1016/j.rse.2016.03.038>, 2016.
- 1151 Obu, J., Westermann, S., Barboux, C., Bartsch, A., Delaloye, R., Grosse, G., Heim, B.,
 1152 Hugelius, G., Irrgang, A., Käab, A. M., Kroisleitner, C., Matthes, H., Nitze, I., Pellet, C., Seifert,

Deleted: :

Deleted: :

Deleted: :

Deleted: :

Deleted: :

Deleted: :

1159 F. M., Strozzi, T., Wegmüller, U., Wieczorek, M., and Wiesmann, A.: ESA permafrost Climate
 1160 Change Initiative (permafrost_cci): Permafrost extent for the Northern Hemisphere, v2.0
 1161 [dataset], <https://doi.org/10.5285/28E889210F884B469D7168FDE4B4E54F>, 2020.

1162 Overeem, I., Nienhuis, J. H., and Piliouras, A.: Ice-dominated Arctic deltas, Nature Reviews
 1163 Earth & Environment, 3, 225-240, <https://doi.org/10.1038/s43017-022-00268-x>, 2022.

1164 Overland, J., Dunlea, E., Box, J. E., Corell, R., Forsius, M., Kattsov, V., Olseng, M. S., Pawlak,
 1165 J., Reiersen, L. O., and Wang, M. Y.: The urgency of Arctic change, Polar Science, 21, 6-13,
 1166 <https://doi.org/10.1016/j.polar.2018.11.008>, 2019.

1167 Pickett, S. T. A., Kolasa, J., Armesto, J. J., and Collins, S. L.: The Ecological Concept of
 1168 Disturbance and Its Expression at Various Hierarchical Levels, Oikos, 54, 129-136,
 1169 <https://doi.org/10.2307/3565258>, 1989.

1170 Piliouras, A. and Rowland, J. C.: Arctic River Delta Morphologic Variability and Implications for
 1171 Riverine Fluxes to the Coast, Journal of Geophysical Research-Earth Surface, 125, ARTN
 1172 e2019JF005250, <https://doi.org/10.1029/2019JF005250>, 2020.

1173 Pisaric, M. F. J., Thienpont, J. R., Kokelj, S. V., Nesbitt, H., Lantz, T. C., Solomon, S., and Smol,
 1174 J. P.: Impacts of a recent storm surge on an Arctic delta ecosystem examined in the context of
 1175 the last millennium, Proceedings of the National Academy of Sciences of the United States of
 1176 America, 108, 8960-8965, <https://doi.org/10.1073/pnas.1018527108>, 2011.

1177 Reynolds, M. K., Walker, D. A., Balser, A., Bay, C., Campbell, M., Cherosov, M. M., Daniels, F.
 1178 J. A., Eidesen, P. B., Emikhina, K. A., Frost, G. V., Jedrzejek, B., Jorgenson, M. T., Kennedy,
 1179 B. E., Kholod, S. S., Lavrinenko, I. A., Lavrinenko, O. V., Magnusson, B., Matveyeva, N. V.,
 1180 Metusalemsson, S., Nilsen, L., Olthof, I., Pospelov, I. N., Pospelova, E. B., Pouliot, D.,
 1181 Razzhivin, V., Schaepman-Strub, G., Sibik, J., Telyatnikov, M. Y., and Troeva, E.: A raster
 1182 version of the Circumpolar Arctic Vegetation Map (CAVM), Remote Sensing of Environment,
 1183 232, ARTN 111297, <https://doi.org/10.1016/j.rse.2019.111297>, 2019.

1184 Romanovskii, N. N. and Hubberten, H. W.: Results of permafrost modelling of the lowlands and
 1185 shelf of the Laptev Sea region, Russia, Permafrost and Periglacial Processes, 12, 191-202,
 1186 <https://doi.org/10.1002/ppp.387>, 2001.

Deleted:],,

Deleted: :

Deleted: :

Deleted: :

Deleted: :

Deleted: :

Deleted: :

Deleted: :

1195 Rossger, N., Sachs, T., Wille, C., Boike, J., and Kutzbach, L.: Seasonal increase of methane
1196 emissions linked to warming in Siberian tundra, *Nature Climate Change*, 12, 1031,
1197 <https://doi.org/10.1038/s41558-022-01512-4>, 2022.

1198 Runge, A., Fuchs, M., Shevtsova, I., Landgraf, N., Heim, B., Herzsuh, U., and Grosse, G.:
1199 Hyperspectral field spectrometry of Arctic vegetation units in the central Lena Delta [dataset],
1200 <https://doi.org/10.1594/PANGAEA.945982>, 2022.

1201 Sachs, T., Wille, C., Boike, J., and Kutzbach, L.: Environmental controls on ecosystem-scale
1202 CH₄ emission from polygonal tundra in the Lena River Delta, Siberia, *Journal of Geophysical*
1203 *Research-Biogeosciences*, 113, Artn G00a03, <https://doi.org/10.1029/2007jg000505>, 2008.

1204 Schirrmeister, L., Grosse, G., Schwamborn, G., Andreev, A. A., Meyer, H., Kunitsky, V. V.,
1205 Kuznetsova, T. V., Dorozhkina, M. V., Pavlova, E. Y., Bobrov, A. A., and Oezen, D.: Late
1206 Quaternary History of the Accumulation Plain North of the Chekanovsky Ridge (Lena Delta,
1207 Russia): A Multidisciplinary Approach, *Polar Geography*, 27, 277-319,
1208 <https://doi.org/10.1080/789610225>, 2003.

1209 Schirrmeister, L., Grosse, G., Schnelle, M., Fuchs, M., Krbetschek, M., Ulrich, M., Kunitsky, V.,
1210 Grigoriev, M., Andreev, A., Kienast, F., Meyer, H., Babiy, O., Klimova, I., Bobrov, A., Wetterich,
1211 S., and Schwamborn, G.: Late Quaternary paleoenvironmental records from the western Lena
1212 Delta, Arctic Siberia, *Palaeogeography Palaeoclimatology Palaeoecology*, 299, 175-196,
1213 <https://doi.org/10.1016/j.palaeo.2010.10.045>, 2011.

1214 Schneider, J., Grosse, G., and Wagner, D.: Land cover classification of tundra environments in
1215 the Arctic Lena Delta based on Landsat 7 ETM+ data and its application for upscaling of
1216 methane emissions, *Remote Sensing of Environment*, 113, 380-391,
1217 <https://doi.org/10.1016/j.rse.2008.10.013>, 2009.

1218 Schwamborn, G., Rachold, V., and Grigoriev, M. N.: Late Quaternary sedimentation history of
1219 the Lena Delta, *Quaternary International*, 89, 119-134, [https://doi.org/10.1016/S1040-](https://doi.org/10.1016/S1040-6182(01)00084-2)
1220 [6182\(01\)00084-2](https://doi.org/10.1016/S1040-6182(01)00084-2), 2002.

1221 Schwamborn, G., Schirrmeister, L., Mohammadi, A., Meyer, H., Kartoziia, A., Maggioni, F., and
1222 Strauss, J.: Fluvial and permafrost history of the lower Lena River, north-eastern Siberia, over
1223 late Quaternary time, *Sedimentology*, 70, 235-258, <https://doi.org/10.1111/sed.13037>, 2023.

Deleted: -+,

Deleted: :

Deleted:],,

Deleted: :

Deleted: :

Deleted: :

Deleted: :

Deleted: :

Deleted: :

1233 Serreze, M. C. and Barry, R. G.: Processes and impacts of Arctic amplification: A research
 1234 synthesis, *Global and Planetary Change*, 77, 85-96,
 1235 <https://doi.org/10.1016/j.gloplacha.2011.03.004>, 2011.

1236 [Siewert, B. M., Hugelius, G., Birgit, H. and Samuel F.: Soil organic carbon storage and soil](#)
 1237 [properties for 50 soil profiles in the Lena River Delta including land form description and map](#)
 1238 [\[dataset publication series\]. PANGAEA, https://doi.org/10.1594/PANGAEA.862961, 2016a](#)

1239 [Siewert, B. M., Hugelius, G., Birgit, H. and Samuel F.: Soil organic carbon \(SOC\) storage in the](#)
 1240 [Lena River Delta \[dataset\]. PANGAEA, https://doi.org/10.1594/PANGAEA.862959, 2016b](#)

1241 [Siewert, B. M., Hugelius, G., Birgit, H. and Samuel F.: Landscape controls and vertical variability](#)
 1242 [of soil organic carbon storage in permafrost-affected soils of the Lena River Delta, CATENA,](#)
 1243 [147, 725-741, https://doi.org/10.1016/j.catena.2016.07.048, 2016c](#)

1244 Shevtsova, I., Laschinskiy, N., Heim, B., and Herzsuh, U.: Foliage projective cover of 26
 1245 vegetation sites of central Lena Delta from 2018 [dataset].
 1246 <https://doi.pangaea.de/10.1594/PANGAEA.935875>, 2021a.

1247 Shevtsova, I., Heim, B., Runge, A., Fuchs, M., Melchert, J., and Herzsuh, U.: Total above-
 1248 ground biomass of 25 vegetation sites of central Lena Delta from 2018 [dataset].
 1249 <https://doi.pangaea.de/10.1594/PANGAEA.935923>, 2021b.

1250 Stanford, J. A., Lorang, M. S., and Hauer, F. R.: The shifting habitat mosaic of river ecosystems,
 1251 *SIL Proceedings*, 1922-2010, 29, 123-136, <https://doi.org/10.1080/03680770.2005.11901979>,
 1252 2005.

1253 Sweeney, C., Chatterjee, A., Wolter, S., McKain, K., Bogue, R., Conley, S., Newberger, T., Hu,
 1254 L., Ott, L., Poulter, B., Schiferl, L., Weir, B., Zhang, Z., and Miller, C. E.: Using atmospheric
 1255 trace gas vertical profiles to evaluate model fluxes: a case study of Arctic-CAP observations and
 1256 GEOS simulations for the ABoVE domain, *Atmospheric Chemistry and Physics*, 22, 6347-6364,
 1257 <https://doi.org/10.5194/acp-22-6347-2022>, 2022.

1258 Ulrich, M., Grosse, G., Chabrilat, S., and Schirrmeister, L.: Spectral characterization of
 1259 periglacial surfaces and geomorphological units in the Arctic Lena Delta using field spectrometry
 1260 and remote sensing, *Remote Sensing of Environment*, 113, 1220-1235,
 1261 <https://doi.org/10.1016/j.rse.2009.02.009>, 2009.

Deleted: :

Deleted:],,

Deleted:],,

Deleted: :

Deleted: :

Deleted: :

- 1268 van Everdingen, R. O.: Multi-language glossary of permafrost and related ground-ice terms,
1269 Arctic Institute of North America University of Calgary, Calgary, [Canada](#), 1998.
- 1270 Veremeeva, A. and Gubin, S.: Modern Tundra Landscapes of the Kolyma Lowland and their
1271 Evolution in the Holocene, Permafrost and Periglacial Processes, 20, 399-406,
1272 <https://doi.org/10.1002/ppp.674>, 2009.
- 1273 Vulis, L., Tejedor, A., Zaliapin, I., Rowland, J. C., and Foufoula-Georgiou, E.: Climate
1274 Signatures on Lake And Wetland Size Distributions in Arctic Deltas, Geophysical Research
1275 Letters, 48, ARTN e2021GL094437, <https://doi.org/10.1029/2021GL094437>, 2021.
- 1276 Walker, H. J.: Arctic deltas, Journal of Coastal Research, 14, 718–738, 1998.
- 1277 Whitaker, R. H. and Woodwell, G. M.: Dimension, and Production Relations of Trees and
1278 Shrubs in the Brookhaven Forest, New York., Journal of Ecology, 56, 1-25,
1279 <https://doi.org/10.1038/2325>, 1968.
- 1280 Zibulski, R., Herzsuh, U., and Pestryakova, L. A.: Vegetation patterns along micro-relief and
1281 vegetation type transects in polygonal landscapes of the Siberian Arctic, Journal of Vegetation
1282 Science, 27, 377-386, <https://doi.org/10.1111/jvs.12356>, 2016.

Deleted: Canada1998

Deleted: :

Deleted: :

Deleted: :

Deleted: :

1283

Figures

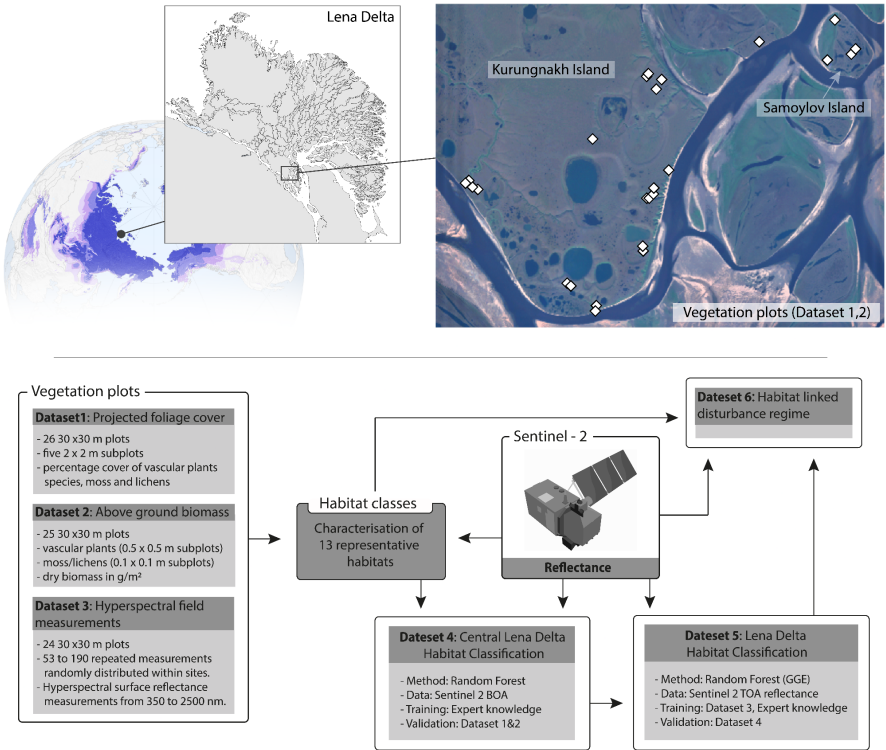
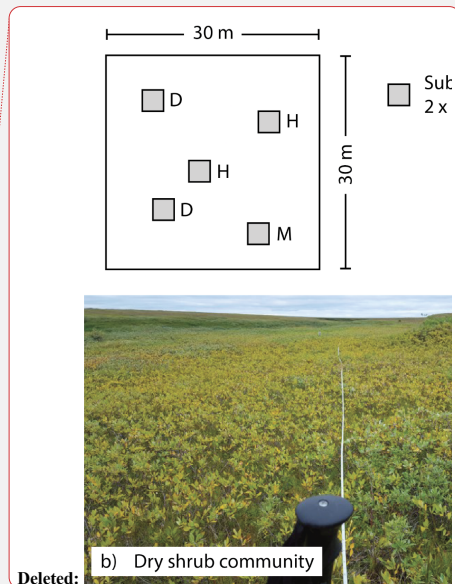
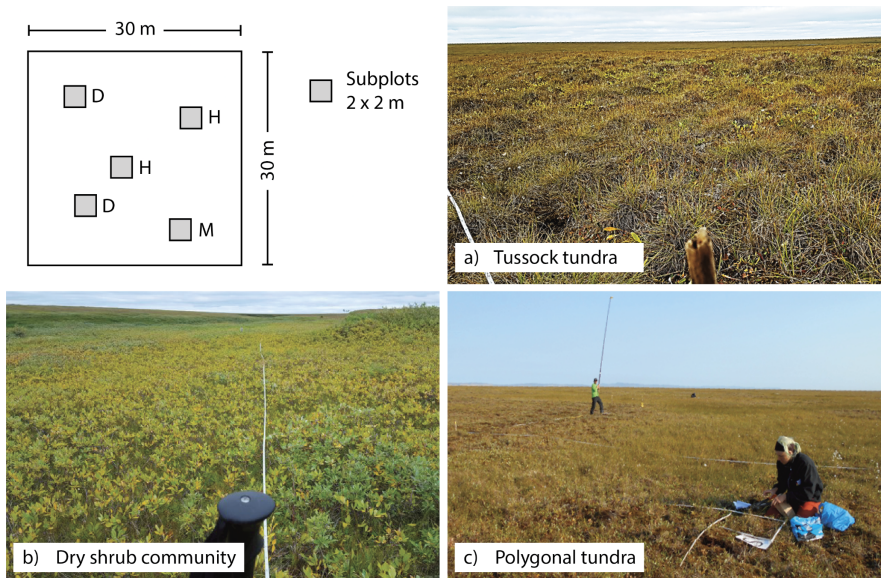


Figure 1: Geographic location of the Lena Delta in the Russian High Arctic (72.91°N, 126.90°E) and a Sentinel-2 RGB image (August 2018, bands 4-3-2) of the central Lena Delta showing the areas of the 26 vegetation plots where foliage projective cover and above ground biomass was determined. Panarctic overview map shows permafrost extent (colour scale indicates permafrost extent from continuous (dark purple) to isolated (light purple) (Obu et al., 2020). The grey-coloured Lena Delta land map created with Sentinel-1 water mask from Juhls et al. (2021). Bottom: Dataset characteristics and methodological links between the different datasets.



1300

1301 Figure 2. Vegetation plots (30 x 30 m) were established in different vegetation types across the
 1302 central Lena Delta. For subplots (2 x 2 m), the projective vegetation cover was recorded and
 1303 labeled according to vegetation and moisture properties (H-Type: homogeneous, M-Type:
 1304 moist, D-Type: dry). Figures illustrate example plots in a) tussock tundra (VP14), b) dry shrub
 1305 communities (VP05), c) polygonal tundra (VP13). Photos: AWI.

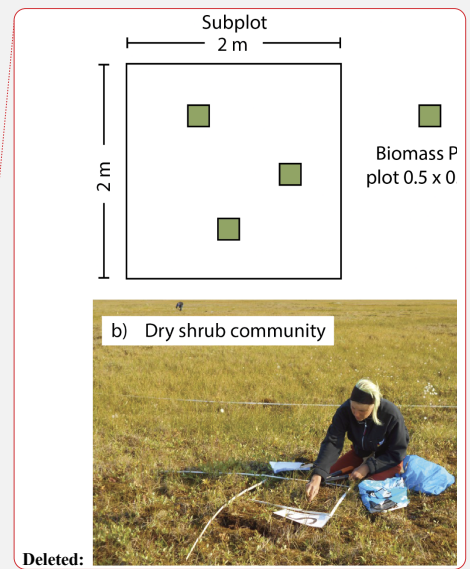
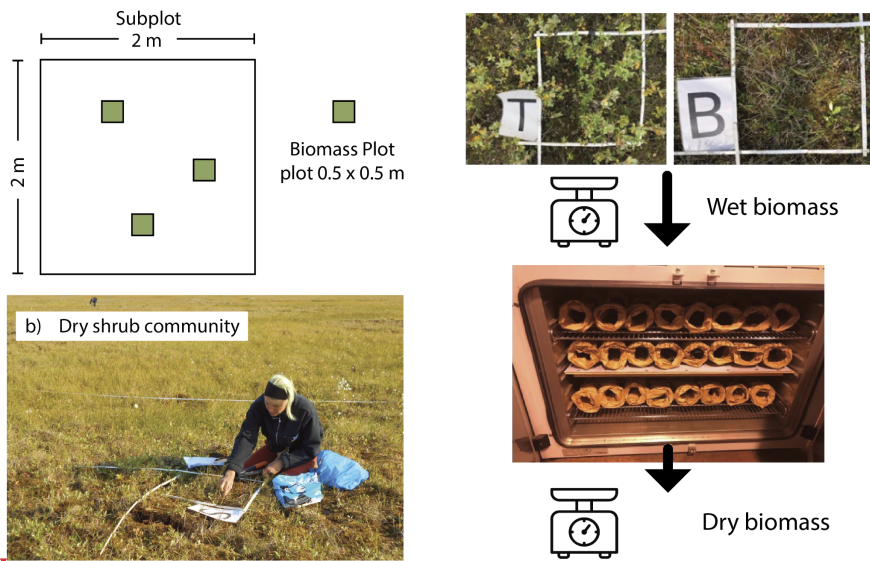
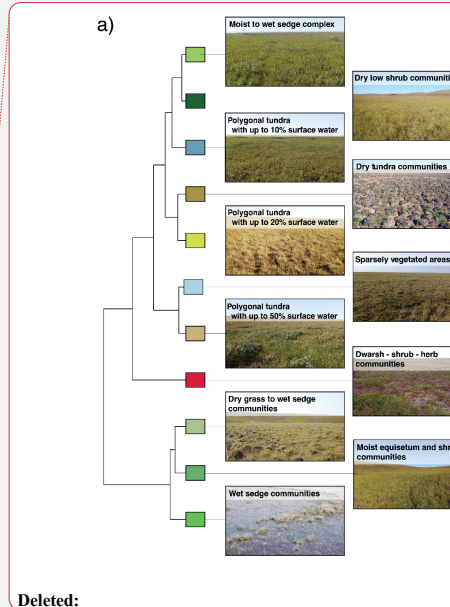
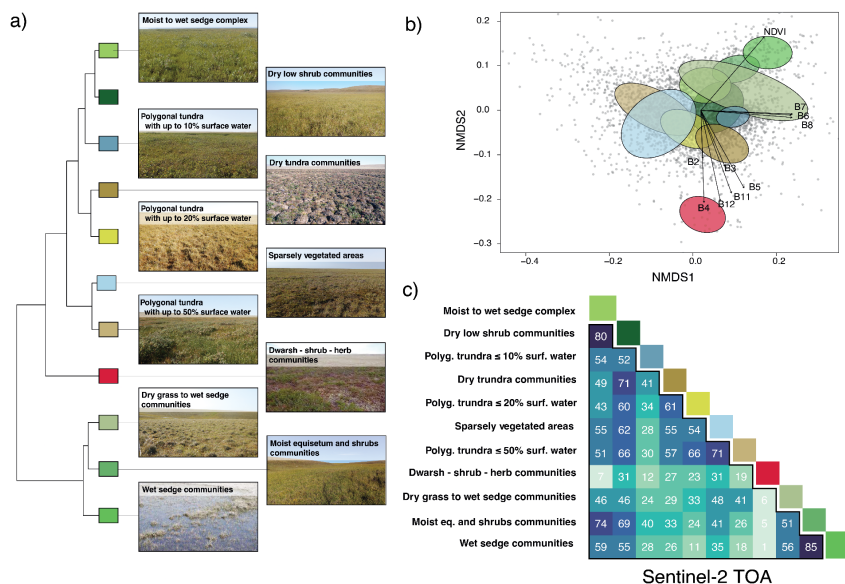
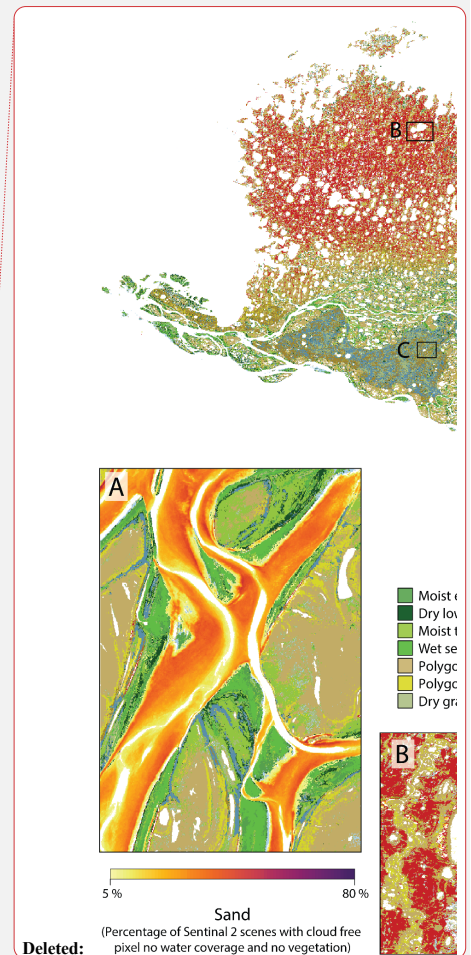
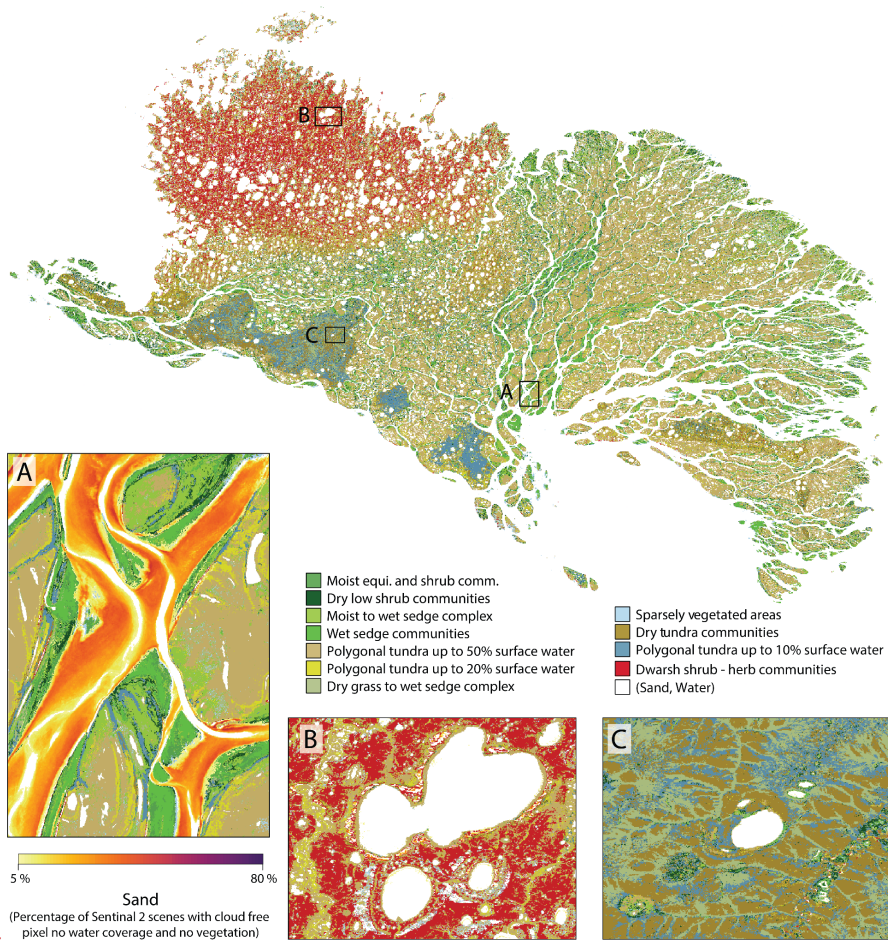
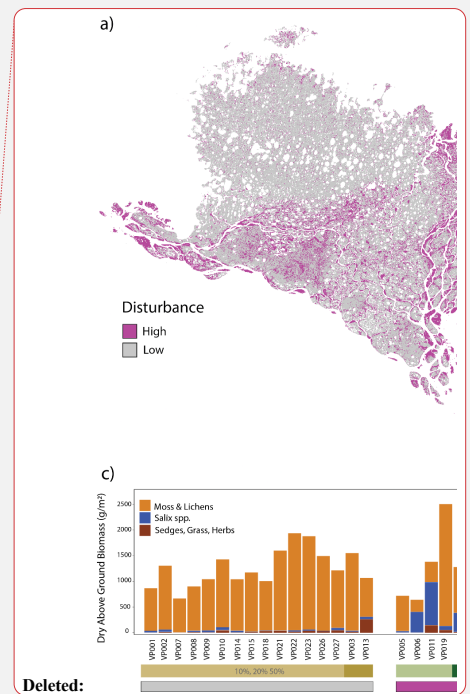
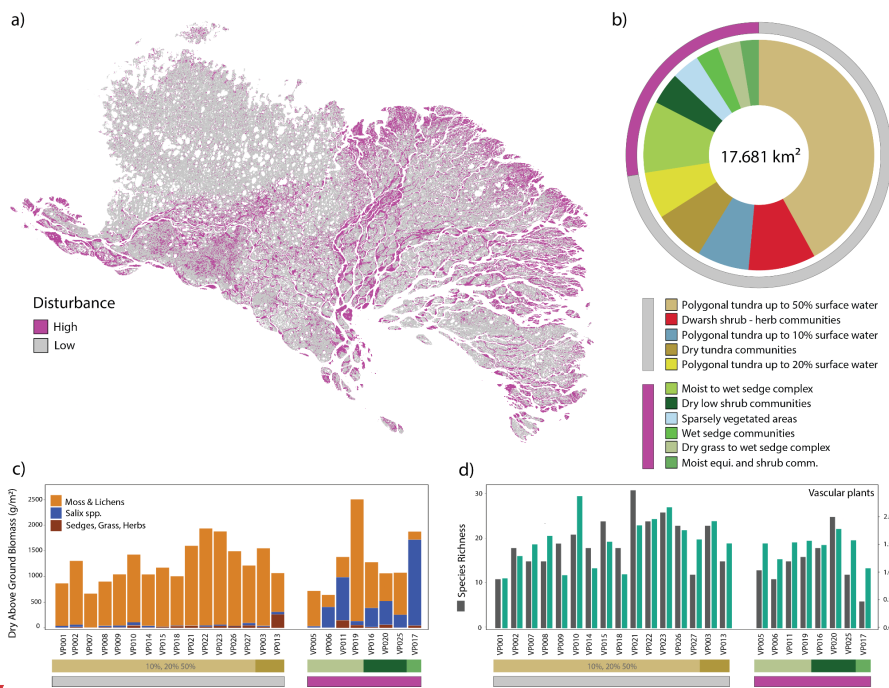


Figure 3. Biomass was sampled in subplots of 0.5 x 0.5 m (and 0.1 x 0.1 m for moss and lichens) distributed within the 2 x 2 m subplots described in Figure 2. Collected plants were weighted (wet biomass), dried in an oven and again weighted (dry biomass). Fotos: AWI.







1336 Tables

1337 Table 1: Habitat classes, descriptions as well as methods used to characterize the distinct
1338 habitats. In-situ vegetation plot numbers correspond to the vegetation plots of Dataset 1 and 2
1339 (see also Table S1, S2, S3).

Habitat types	Description	Method
Moist <i>Equisetum</i> and shrubs	<i>Equisetum</i> and shrub communities form an early-to-middle successional stage growing on the active floodplain. Low moss contribution	In-situ vegetation plot (VP17); extended to representative larger polygon shape files using field knowledge.
Dry shrub communities	Patch forming shrub communities dominated by dwarf willow (<i>Salix</i>) thickets, frequently occurring on dry elevated areas on floodplains and stream floodplains and in topographically sheltered areas below basin and valley rims. Low moss contribution	In-situ vegetation plots (VP04, VP16); extended to representative larger polygon shape files using field knowledge.
Polygonal tundra complex up to - 10% - 20% - 50% surface water (3 distinct classes)	Mature-state plant communities dominated by sedge, moss and herb species. Sparse vascular plant coverage (dwarf willows, dwarf birches) on thick continuous moss cover. Occurring on the plateaus of the ice-rich holocene and pleistocene terraces, and at the bottom of alases. Intersected by intra- and interpolygonal ponds resulting in up to 10%, 20%, 50% surface water contribution.	In-situ vegetation plots (VP01, VP02, VP07, VP08, VP14, VP15, VP18, VP21, VP22, VP23, VP26, VP27); extended to representative larger polygon shape files using field knowledge. The different surface water contributions were defined based on the result from unsupervised classification.
Dry grass to wet sedge communities	These early-to-middle successional plant communities cover unstable valley slopes and a young drained lake basin, they are mostly composed of sedges and grasses, but also willows (<i>Salix</i>) are part of this habitat.	In-situ vegetation plots (VP05, VP06, VP11, VP19, VP20); extended to representative larger polygon shape files using field knowledge.
Dry tundra communities	The mature-state dry tundra communities represent the zonal tundra type, one subclass is dominated by tussock forming <i>Eriophorum</i> and the other by less tussock forming dry-herb communities, dominated by <i>Dryas</i> . Occurring on well-drained slopes of valleys and alases, and other well-drained areas on the terraces. High moss contribution	In-situ vegetation plots (VP03, VP13) extended to representative, larger polygon shape files using field knowledge (including 'dry tundra communities type tussock' and 'dry tundra communities').
Moist to wet sedge communities	These mid to advanced successional plant communities occur on moist to water-logged soils characteristically mostly in topographic depressions on the floodplains, in valleys and alases. They constitute the rims of the wetland areas on	Polygon shape files derived from high resolution satellite image and ESRI GE with regional expert knowledge. No vegetation plots (too wet).

Deleted: a

	the floodplains in more dynamic parts the moss ground cover is missing.	
Wet sedge communities	These mid to advanced successional plant communities occur at permanently wet sites with stagnant water in the topographic depressions and are typical for wetland areas on the floodplains. In more dynamic parts the moss ground cover is missing.	Polygon shape files derived from high resolution satellite image and ESRI GE with regional expert knowledge. No vegetation plots (too wet).
Sparsely vegetated areas	These early successional plant communities are characterized by low vegetation establishment and coverage. No to low moss contribution	Defined based on the result from unsupervised classification, polygon shape files. No vegetation plots.
Barren/Sand	Representing the wide-open sand flats of the floodplain and barren ground on valley slopes or along cliffs. In a few cases, this class represents vegetation-free bedrock outcrops.	Threshold using high reflectance in S2-band 2 blue.
Water	Represents all surface water bodies in the delta: the Lena River with river branches, streams, lakes and large ponds.	Threshold using low reflectance in S2-band 8 NIR.

1341

1342 Table 2: Habitat class and description of disturbance regimes and the component stand
 1343 structure in form of contributions of vascular plants, and moss to total biomass. * (Driscoll and
 1344 Hauer, 2019; Stanford et al., 2005), ** (Lorang and Hauer, 2006).

Habitat class	Disturbance regime	Stand structure
Moist <i>Equisetum</i> and shrubs	High; regular (annually), predicted - spring floodings, - shifting habitat * - advanced-stage regeneration **	high vascular plant growth, low abundance of moss & lichens.
Dry shrub communities	High; mixed disturbance types: - regular spring floodings - rapid thaw processes (permafrost degradation) - shifting habitat - advanced-stage regeneration	high vascular plant growth, low abundance of moss.
Polygonal tundra complex	Low; mixed disturbance types - low for most of the habitat, except for actively eroding shores of ponds and channels - mature-state plant community	low vascular plant growth, high abundance of moss.
Dry grass to wet sedge communities	High; mixed disturbance types: - regular spring floodings - rapid thaw processes (permafrost degradation) - shifting habitat - advanced-stage regeneration	high vascular plant biomass, low abundance of moss.
Dry tundra communities	Low; mixed disturbance types - low for most of the habitat - mature-state plant community	low vascular plant biomass high abundance of moss.
Moist to wet sedge communities	High; mixed disturbance types: - regular spring floodings - rapid thaw processes (permafrost degradation) - shifting habitat - mid to advanced-stage regeneration	high vascular plant biomass Almost impossible to measure in-situ biomass (wet conditions and difficult access).
Wet sedge communities	High; mixed disturbance types: - regular spring floodings - rapid thaw processes (permafrost degradation) - shifting habitat - mid to advanced-stage regeneration	high vascular plant biomass. Almost impossible to measure in-situ biomass (wet conditions and difficult access).
Dwarf shrub herb communities	Low; mixed disturbance types - low for most of the habitat - mature-state plant community	low vascular plant biomass, high abundance of moss.
Sparsely vegetated areas	Very high; mixed disturbance types - regular spring floodings	lowest vascular plant biomass, no moss.

	<ul style="list-style-type: none"> - rapid thaw processes (permafrost degradation) - shifting habitat - early-stage regeneration 	
Sand banks/barren	Very high: mixed disturbance types <ul style="list-style-type: none"> - regular spring floodings - rapid thaw processes (permafrost degradation) - shifting habitat - no regeneration 	Barren, constant shifting of sediments and movement of soils.

1345

Page 25: [1] Deleted Cells	Simeon Lisovski	31/01/2025 15:15:00
Deleted Cells		
Page 25: [2] Deleted Cells	Simeon Lisovski	31/01/2025 15:15:00
Deleted Cells		
Page 25: [3] Inserted Cells	Simeon Lisovski	31/01/2025 15:15:00
Inserted Cells		
Page 25: [4] Inserted Cells	Simeon Lisovski	31/01/2025 15:15:00
Inserted Cells		
Page 25: [5] Inserted Cells	Simeon Lisovski	31/01/2025 15:15:00
Inserted Cells		
Page 25: [6] Inserted Cells	Simeon Lisovski	31/01/2025 15:15:00
Inserted Cells		
Page 25: [7] Inserted Cells	Simeon Lisovski	31/01/2025 15:15:00
Inserted Cells		
Page 25: [8] Inserted Cells	Simeon Lisovski	31/01/2025 15:15:00
Inserted Cells		
Page 25: [9] Inserted Cells	Simeon Lisovski	31/01/2025 15:15:00
Inserted Cells		
Page 25: [10] Deleted Cells	Simeon Lisovski	31/01/2025 15:15:00
Deleted Cells		
Page 25: [11] Deleted Cells	Simeon Lisovski	31/01/2025 15:15:00
Deleted Cells		
Page 25: [12] Inserted Cells	Simeon Lisovski	31/01/2025 15:15:00
Inserted Cells		
Page 25: [13] Inserted Cells	Simeon Lisovski	31/01/2025 15:15:00
Inserted Cells		
Page 25: [14] Deleted	Simeon Lisovski	31/01/2025 15:15:00

▼